Available online at www.sciencedirect.com

SCIENCE DIRECT

Virology 331 (2005) 269–291

VIROLOGY

www.elsevier.com/locate/yviro

Gene expression profiles of primary HPV16- and HPV18-infected early stage cervical cancers and normal cervical epithelium: identification of novel candidate molecular markers for cervical cancer diagnosis and therapy

Alessandro D. Santin[a,*], Fenghuang Zhan[b], Eliana Bignotti[a], Eric R. Siegel[c], Stefania Cané[a], Stefania Bellone[a], Michela Palmieri[a], Simone Anfossi[a], Maria Thomas[d], Alexander Burnett[a], Helen H. Kay[e], Juan J. Roman[a], Timothy J. O'Brien[a], Erming Tian[b], Martin J. Cannon[f], John Shaughnessy Jr.[b], Sergio Pecorelli[g]

[a]*Division of Gynecologic Oncology, University of Arkansas for Medical Sciences, Little Rock, AR 72205, USA*
[b]*Myeloma Institute for Research and Therapy, University of Arkansas for Medical Sciences, Little Rock, AR 72205, USA*
[c]*Department of Biostatistics, University of Arkansas for Medical Sciences, Little Rock, AR 72205, USA*
[d]*Department of Pathology, University of Arkansas for Medical Sciences, Little Rock, AR 72205, USA*
[e]*Department of Obstetrics and Gynecology, University of Arkansas for Medical Sciences, Little Rock, AR 72205, USA*
[f]*Department of Microbiology and Immunology, University of Arkansas, Little Rock, AR 72205, USA*
[g]*Division of Gynecologic Oncology, University of Brescia, Brescia, Italy*

Received 2 July 2004; returned to author for revision 18 August 2004; accepted 9 September 2004
Available online 21 November 2004

Abstract

With the goal of identifying genes with a differential pattern of expression between invasive cervical carcinomas (CVX) and normal cervical keratinocytes (NCK), we used oligonucleotide microarrays to interrogate the expression of 14,500 known genes in 11 primary HPV16 and HPV18-infected stage IB–IIA cervical cancers and four primary normal cervical keratinocyte cultures. Hierarchical cluster analysis of gene expression data identified 240 and 265 genes that exhibited greater than twofold up-regulation and down-regulation, respectively, in primary CVX when compared to NCK. Cyclin-dependent kinase inhibitor 2A (CDKN2A/p16), mesoderm-specific transcript, forkhead box M1, v-myb myeloblastosis viral oncogene homolog (avian)-like2 (v-Myb), minichromosome maintenance proteins 2, 4, and 5, cyclin B1, prostaglandin E synthase (PTGES), topoisomerase II alpha (TOP2A), ubiquitin-conjugating enzyme E2C, CD97 antigen, E2F transcription factor 1, and dUTP pyrophosphatase were among the most highly overexpressed genes in CVX when compared to NCK. Down-regulated genes in CVX included transforming growth factor beta 1, transforming growth factor alpha, CFLAR, serine proteinase inhibitors (SERPING1 and SERPINF1), cadherin 13, protease inhibitor 3, keratin 16, and tissue factor pathway inhibitor-2 (TFPI-2). Differential expression of some of these genes including *CDKN2A/p16*, *v-Myb*, *PTGES*, and *TOP2A* was validated by quantitative real-time PCR. Flow cytometry on primary CVX and NCK and immunohistochemical staining of formalin fixed paraffin-embedded tumor specimens from which primary CVX cultures were derived as well as from a separate set of invasive cervical cancers confirmed differential expression of the *CDKN2A/p16* and *PTGES* markers on CVX versus NCK. These results identify several genes that are coordinately disregulated in cervical cancer, likely representing common signaling pathways triggered by HPV transformation. Moreover, these data obtained with highly purified primary tumor cultures highlight novel molecular features of

Abbreviations: CVX, invasive cervical carcinomas; NCK, normal cervical keratinocytes.

* Corresponding author. UAMS Medical Center, Department of Obstetrics and Gynecology, 4301 West Markham, slot 518, Little Rock, AR 72205-7199, USA. Fax: +1 501 686 8091.
E-mail address: santinalessandrod@uams.edu (A.D. Santin).

0042-6822/$ - see front matter
doi:10.1016/j.virol.2004.09.045

human cervical cancer and provide a foundation for the development of new type-specific diagnostic and therapeutic strategies for this disease.

Keywords: Cervical cancer; Human papillomavirus; Gene expression profiling

Introduction

Cervical cancer remains the second-most common cause of cancer-related deaths in women worldwide, with about 450,000 new cases diagnosed each year (Bosch et al., 2002; Jemal et al., 2003). Human papillomavirus (HPV) infection represents the most important risk factor for the development of cervical cancer (Bosch et al., 2002). Prevalence surveys, large case-control studies, and case series have unequivocally shown that HPV DNA can be detected in cervical cancer specimens in 90–100% of cases, compared with a prevalence of 5–20% in cervical specimens from women identified as suitable epidemiological controls (Bosch et al., 2002). Although more than 100 distinct HPV genotypes have been described, and at least 20 are associated with cervical cancer, HPV types 16 and 18 are the most frequently detected in cervical cancer regardless of the geographical origin of the patients (Bosch et al., 2002). Although early stage cervical cancer can be cured by radical surgery or radiotherapy with equal effectiveness (Landoni et al., 1997), pelvic radiation represents the standard therapy for the treatment of locally advanced disease. Despite technological advances, however, up to 35% of patients overall will develop advanced, metastatic disease, for which treatment results are poor. A deeper understanding of the molecular basis of cervical cancer has the potential to refine significantly the diagnosis and management of these tumors and may eventually lead to the development of novel, more specific and more effective treatments for prevention of disease progression following first-line therapy.

High-throughput comprehensive technologies for assaying gene expression, such as high-density oligonucleotide and cDNA microarrays, have recently been used in an attempt to identify genes changes in keratinocytes associated with high-risk HPV infection and thus involved in cervical carcinogenesis (Alazawi et al., 2002; Chang and Laimins, 2000; Chen et al., 2003; Nees et al., 2001; Oh et al., 2001). However, global gene expression studies related to cervical cancer have so far been limited to investigations of in vitro HPV-transfected human keratinocytes (Chang and Laimins, 2000; Nees et al., 2001; Oh et al., 2001), cervical low-grade squamous intraepithelial lesions (Alazawi et al., 2002), or snap-frozen tumor biopsies (Chen et al., 2003). In this study, we used oligonucleotide microarrays containing more than 22,000 unique transcripts to analyze the gene expression profiles of 15 primary cervical cell lines [i.e., 11 primary HPV16- or HPV18-positive cervical cancer cultures (CVX) derived from early stage disease and four normal cervical keratinocyte cell lines (NCK)]. Short-term primary CVX and NCK cell cultures, which minimize the risk of a selection bias inherent in any long-term in vitro growth, provide an opportunity to study differential gene expression between highly enriched and homogeneous populations of tumors and normal cervical-derived epithelial cells.

We report that mRNA fingerprints readily distinguish CVX from NCK and identify a number of genes highly differentially expressed between nontransformed keratinocytes and invasive cervical cancer. Some of the genes identified are already known to be overexpressed in cervical cancer and to play crucial roles during HPV carcinogenesis, validating our criteria for determination of differentially expressed genes, but many other variably expressed genes represent novel findings. Quantitative RT-PCR was used to validate differences in gene expression between CVX and NCK for some of these genes, including cyclin-dependent kinase inhibitor 2A (*CDKN2A*), v-myb myeloblastosis viral oncogene homolog (avian)-like 2 (*v-Myb*), prostaglandin E synthase (*PTGES*), and topoisomerase (*TOP2A*). The gene expression product of *CDKN2A* (i.e., p16) was further validated through flow cytometric analysis of primary CVX and NCK and by immunohistochemical analysis of formalin-fixed paraffin-embedded specimens from which primary CVX cultures were derived as well as from a separate and independent set of invasive cervical cancer specimens.

Results

Gene expression profiles distinguish CVX from NCK and identify differentially expressed genes

Flash-frozen biopsies from cervical tumor tissue and normal cervix may contain significant numbers of contaminant stromal cells as well as a variety of host-derived immune cells (e.g., monocytes, dendritic cells, lymphocytes). In addition, because early stage cervical cancer epithelial cells may represent a small proportion of the total cells found in the cervix, it is often difficult to collect primary material that is free of contaminating cells in sufficient quantities to conduct comparative gene expression analyses. Short-term primary CVX and NCK cultures, which minimize the risk of a selection bias inherent in any long-term in vitro growth, may provide an opportunity to

study differential gene expression between highly enriched populations of normal and tumor-derived epithelial cells. Accordingly, comprehensive gene expression profiles of 11 primary CVX and four primary NCK cell lines were generated using high-density oligonucleotide arrays with 22,215 probe sets, which in total interrogated some 14,500 genes. Out of the 22,215 probe sets, a total of 1354 showed both a greater than twofold change between groups and detection = present calls in more than half of the samples. The WRS test at level alpha = 0.05 revealed that 982 of these expression changes were statistically significant. Because the WRS test is a rank test, only seven discrete WRS *P* values occur at or below alpha = 0.05. For each *P* value, Table 1 shows the number of genes discovered and 99% confidence maxima on the percentage of discoveries that are false. At a WRS *P* value of 0.009, the cumulative gene total was 505 with a 99% confidence maximum of 20.48 false discoveries (4.05%). Of these 505 genes with WRS $P < 0.01$, 240 showed up-regulation and 265 showed down-regulation in CVX over NCK. The cluster analysis performed on hybridization intensity values for the 505 gene segments just described is shown in Fig. 1. All four NCK were grouped together in the leftmost columns. Similarly, in the rightmost columns all 11 CVX were found to cluster together. The tight clustering of CVX from NCK was "driven" by two distinct profiles of gene expression. The first was represented by a group of 240 genes that were highly expressed in CVX and underexpressed in NCK (Table 2). Genes shown previously to be involved in cervical carcinogenesis are present on this list, providing some validity to our array analysis, while others are novel in cervical carcinogenesis. Included in this group of genes are cyclin-dependent kinase inhibitor 2A (*CDKN2A/p16*), mesoderm-specific transcript (*MEST*), forkhead box M1 (*FOXM1*), v-myb myeloblastosis viral oncogene homolog (avian)-like 2, prostaglandin E synthase (*PTGES*), minichromosome maintenance proteins (*MCM*) 2, 4, and 5,

Table 1
False discoveries among differentially expressed genes

WRS[a] *P* value	Number[b] of genes discovered	Percent false discoveries[c] (%)
0.0041	241	4.61
0.0061	361	4.18
0.0090	505	4.05
0.0131	632	4.38
0.0188	773	4.81
0.0265	876	5.68
0.0367	982	6.72

[a] Wilcoxon rank-sum test with normal approximation, applied to 1354 genes showing >2× change between groups and present calls >50% in the higher expressing group.
[b] Number having WRS *P* value less than or equal to indicated value.
[c] 99%-Confidence Maximum on Number of False Discoveries expressed as a percent of the Number of Genes Discovered, given that 1354 genes were tested via WRS.

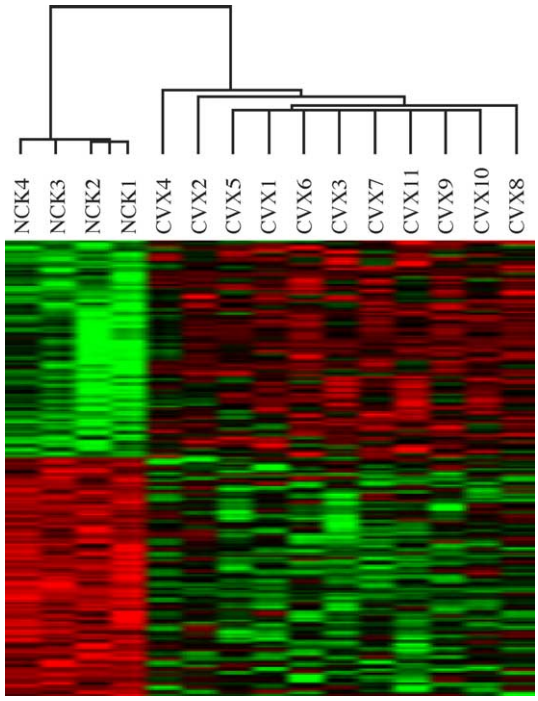

Fig. 1. Hierarchical clustering of 505 genes with differential expression between 11 CVX and 4 NCK groups ($P < 0.01$) using a twofold threshold. The cluster is color coded using red for up-regulation, green for down-regulation, and black for median expression. Agglomerative clustering of genes is illustrated with dendrograms.

cyclin B1, topoisomerase II alpha (*TOP2A*), ubiquitin-conjugating enzyme E2C, CD97 antigen, E2F transcription factor 1, catenin-beta, and dUTP pyrophosphatase (Table 2). The second profile was represented by 265 genes that were highly expressed in NCK and underexpressed in CVX (Table 3). Included in this group of genes are differentiation-related genes and tumor suppressor genes including transforming growth factor, beta 1, transforming growth factor alpha, CFLAR, serine proteinase inhibitors (*SERPING1* and *SERPINF1*), cadherin 13, protease inhibitor 3, and keratin 16.

Validation of the microarray data

We used q-RT-PCR assays to validate the microarray data. Four highly differentially expressed genes between CVX and NCK (i.e., *CDKN2A*, *v-Myb*, *PTGES*, and *TOP2A)* were selected for q-RT-PCR analysis. A comparison of the microarray and q-RT-PCR data for these genes is shown in Fig. 2. Expression differences between CVX and NCK for *CDKN2A/p16* ($P = 0.002$), *v-Myb* ($P = 0.03$), *PTGES* ($P = 0.03$), and *TOP2A* ($P = 0.02$) were readily apparent (Table 2 and Fig. 2). Moreover, qRT-PCR data were significantly correlated to microarray data for the above four genes, as determined by Spearman rank correlation as follows: *CDKN2A/p16* ($s = 0.5393$, $P = 0.0380$); *v-Myb* ($s = 0.8101$, $P = 0.0003$); *PTGES* ($s = 0.8136$, $P = 0.0002$); and *TOP2A* ($s = 0.6357$, $P =$

Table 2
Up-regulated genes expressed at least twofold higher in CVX compared with NCK

U133A probe set	Gene symbol	WRS *P* value	Average for CVX	Ratio CVX/NCK	Activity or Description
205081_at	CRIP1	0.004075	1662.5	105.39	cysteine-rich protein 1 (intestinal)
207069_s_at	MADH6	0.009023	221.5	18.62	MAD, mothers against decapentaplegic homolog 6 (*Drosophila*)
221436_s_at	GRCC8	0.004075	1150.3	11.46	likely ortholog of mouse gene-rich cluster, C8 gene
208510_s_at	PPARG	0.006112	365.4	10.54	peroxisome proliferative activated receptor, gamma
209644_x_at	CDKN2A	0.004075	7829.7	10.05	cyclin-dependent kinase inhibitor 2A (melanoma, p16, inhibits CDK4)
204560_at	FKBP5	0.004075	525.3	9.50	FK506 binding protein 5
206858_s_at	HOXC6	0.009023	498.4	9.11	homeobox C6
207039_at	CDKN2A	0.004075	2616.4	9.05	cyclin-dependent kinase inhibitor 2A (melanoma, p16, inhibits CDK4)
202016_at	MEST	0.004075	2220.9	7.99	mesoderm-specific transcript homolog (mouse)
218959_at	HOXC10	0.009023	850.3	7.46	homeobox C10
202580_x_at	FOXM1	0.004075	1624.4	7.42	forkhead box M1
201710_at	MYBL2	0.004075	1458.0	6.71	v-myb myeloblastosis viral oncogene homolog (avian)-like 2
203276_at	LMNB1	0.006112	496.7	6.59	lamin B1
204766_s_at	NUDT1	0.006112	442.3	6.58	nudix (nucleoside diphosphate linked moiety X)-type motif 1
204641_at	NEK2	0.004075	667.3	6.42	NIMA (never in mitosis gene a)-related kinase 2
201291_s_at	TOP2A	0.009023	505.9	6.38	topoisomerase (DNA) II alpha 170 kDa
216212_s_at	DKC1	0.009023	978.5	6.31	dyskeratosis congenita 1, dyskerin
201970_s_at	NASP	0.009023	1358.5	6.14	nuclear autoantigenic sperm protein (histone-binding)
219978_s_at	ANKT	0.004075	990.0	6.08	nucleolar protein ANKT
207388_s_at	PTGES	0.004075	2539.5	5.99	prostaglandin E synthase
213008_at	FLJ10719	0.006112	429.0	5.89	hypothetical protein FLJ10719
205862_at	GREB1	0.006112	54.8	5.75	GREB1 protein
212141_at	MCM4	0.004075	1137.1	5.59	MCM4 minichromosome maintenance deficient 4 (*S. cerevisiae*)
201774_s_at	CNAP1	0.004075	1672.0	5.54	chromosome condensation-related SMC-associated protein 1
218039_at	ANKT	0.006112	2027.1	5.54	nucleolar protein ANKT
210052_s_at	C20orf1	0.004075	2786.1	5.51	chromosome 20 open reading frame 1
202954_at	UBE2C	0.006112	4354.1	5.23	ubiquitin-conjugating enzyme E2C
210367_s_at	PTGES	0.004075	3098.6	5.20	prostaglandin E synthase
202910_s_at	CD97	0.004075	495.6	5.02	topoisomerase (DNA) II alpha
208079_s_at	STK6	0.004075	1915.1	4.93	serine/threonine kinase 6
203418_at	CCNA2	0.009023	1013.0	4.85	cyclin A2
209714_s_at	CDKN3	0.004075	1327.1	4.84	cyclin-dependent kinase inhibitor 3 (CDK2-associated dual specificity phosphatase)
218755_at	RAB6KIFL	0.006112	1015.1	4.83	RAB6 interacting, kinesin-like (rabkinesin6)
218009_s_at	PRC1	0.006112	2515.3	4.81	protein regulator of cytokinesis 1
204317_at	–	0.004075	163.0	4.80	unknown (protein for MGC:15422) (*Homo sapiens*), mRNA sequence
218741_at	MGC861	0.004075	889.6	4.71	hypothetical protein MGC861
202705_at	CCNB2	0.004075	2283.1	4.61	cyclin B2
219555_s_at	BM039	0.006112	798.7	4.59	uncharacterized bone marrow protein BM039
204233_s_at	CHK	0.004075	480.9	4.59	choline kinase
202251_at	HPRP3P	0.004075	493.1	4.55	U4/U6-associated RNA splicing factor
202107_s_at	MCM2	0.006112	5267.9	4.55	MCM2 minichromosome maintenance deficient 2, mitotin (*S. cerevisiae*)
213599_at	OIP5	0.004075	887.8	4.53	Opa-interacting protein 5
201755_at	MCM5	0.009023	1058.4	4.53	MCM5 minichromosome maintenance deficient 5, cell division cycle 46 (*S. cerevisiae*)
221206_at	-	0.009023	373.4	4.50	
212552_at	HPCAL1	0.004075	4490.3	4.49	hippocalcin-like 1
204827_s_at	CCNF	0.004075	263.1	4.48	cyclin F
222039_at	(EST)	0.006112	1031.2	4.37	ESTs, moderately similar to PRO0478 protein (*H. sapiens*)
202870_s_at	CDC20	0.004075	3250.6	4.36	CDC20 cell division cycle 20 homolog (*S. cerevisiae*)
205462_s_at	HPCAL1	0.004075	1501.7	4.35	hippocalcin-like 1

Table 2 (*continued*)

U133A probe set	Gene symbol	WRS *P* value	Average for CVX	Ratio CVX/NCK	Activity or Description
203967_at	CDC6	0.009023	1133.1	4.22	CDC6 cell division cycle 6 homolog (*S. cerevisiae*)
214710_s_at	CCNB1	0.006112	2481.4	4.21	cyclin B1
202589_at	TYMS	0.009023	5175.0	4.17	thymidylate synthetase
204023_at	RFC4	0.004075	2093.9	4.14	replication factor C (activator 1) 4, 37 kDa
204092_s_at	STK6	0.006112	1858.6	4.13	serine/threonine kinase 6
208072_s_at	DGKD	0.004075	552.5	4.10	diacylglycerol kinase, delta 130 kDa
201663_s_at	SMC4L1	0.009023	669.9	4.06	SMC4 structural maintenance of chromosomes 4-like 1 (yeast)
204947_at	E2F1	0.006112	517.9	4.05	E2F transcription factor 1
204962_s_at	CENPA	0.004075	741.6	4.02	centromere protein A, 17 kDa
202976_s_at	RHOBTB3	0.009023	442.0	4.00	Rho-related BTB domain containing 3
219143_s_at	FLJ20374	0.009023	997.9	3.95	hypothetical protein FLJ20374
204709_s_at	KNSL5	0.009023	134.2	3.91	kinesin-like 5 (mitotic kinesin-like protein 1)
202095_s_at	BIRC5	0.006112	1538.6	3.90	baculoviral IAP repeat-containing 5 (survivin)
212282_at	MAC30	0.004075	1940.1	3.84	hypothetical protein MAC30
210004_at	OLR1	0.009023	217.5	3.84	oxidized low-density lipoprotein (lectin-like) receptor 1
213610_s_at	–	0.009023	123.3	3.84	unknown (protein for IMAGE:3354344) (*H. sapiens*), mRNA sequence
208161_s_at	ABCC3	0.006112	608.0	3.77	ATP binding cassette, subfamily C (CFTR/MRP), member 3
209406_at	BAG2	0.004075	583.6	3.76	BCL2-associated athanogene 2
216237_s_at	MCM5	0.009023	2762.4	3.68	MCM5 minichromosome maintenance deficient 5, cell division cycle 46 (*S. cerevisiae*)
209172_s_at	CENPF	0.004075	149.8	3.68	centromere protein F, 350/400 kDa (mitosin)
210206_s_at	DDX11	0.006112	352.0	3.66	DEAD/H (Asp-Glu-Ala-Asp/His) box polypeptide 11 (CHL1-like helicase homolog, *S. cerevisiae*)
202240_at	PLK	0.004075	980.0	3.64	polo-like kinase (*Drosophila*)
202094_at	BIRC5	0.009023	577.0	3.63	baculoviral IAP repeat-containing 5 (survivin)
203046_s_at	TIMELESS	0.004075	823.7	3.63	timeless homolog (*Drosophila*)
212621_at	KIAA0286	0.009023	578.0	3.61	KIAA0286 protein
208103_s_at	LANPL	0.009023	507.6	3.60	leucine-rich acidic nuclear protein-like
203432_at	(EST)	0.006112	1461.0	3.58	ESTs
219512_at	C20orf172	0.009023	215.8	3.56	chromosome 20 open reading frame 172
204026_s_at	ZWINT	0.006112	2673.5	3.54	ZW10 interactor
221591_s_at	FLJ10156	0.009023	757.7	3.49	hypothetical protein FLJ10156
203968_s_at	CDC6	0.006112	941.6	3.48	CDC6 cell division cycle 6 homolog (*S. cerevisiae*)
202779_s_at	E2-EPF	0.004075	8293.5	3.45	ubiquitin carrier protein
204033_at	TRIP13	0.006112	1741.5	3.44	thyroid hormone receptor interactor 13
203832_at	SNRPF	0.006112	3153.1	3.43	small nuclear ribonucleoprotein polypeptide F
217821_s_at	WBP11	0.004075	1204.5	3.43	WW domain binding protein 11
211450_s_at	MSH6	0.006112	891.7	3.43	mutS homolog 6 (*Escherichia coli*)
216669_at	(FLJ20286)	0.006112	63.2	3.42	*H. sapiens* cDNA FLJ20286 fis, clone HEP04358, mRNA sequence
204822_at	TTK	0.006112	474.0	3.41	TTK protein kinase
219502_at	FLJ10858	0.004075	392.4	3.37	hypothetical protein FLJ10858
203145_at	SPAG5	0.006112	762.0	3.36	sperm-associated antigen 5
219588_s_at	FLJ20311	0.006112	802.2	3.34	hypothetical protein FLJ20311
203625_x_at	(FLJ22571)	0.009023	1085.2	3.34	*H. sapiens* cDNA: FLJ22571 fis, clone HSI02239, mRNA sequence
205167_s_at	CDC25C	0.004075	366.2	3.32	cell division cycle 25C
204147_s_at	TFDP1	0.004075	667.9	3.31	transcription factor Dp-1
213906_at	MYBL1	0.006112	161.6	3.31	v-myb myeloblastosis viral oncogene homolog (avian)-like 1
215116_s_at	DNM1	0.006112	693.9	3.28	dynamin 1
212281_s_at	MAC30	0.004075	1879.4	3.22	hypothetical protein MAC30
201897_s_at	CKS1B	0.006112	4568.0	3.21	CDC28 protein kinase regulatory subunit 1B
221648_s_at	(FLJ21998)	0.004075	399.9	3.19	*H. sapiens* cDNA: FLJ21998 fis, clone HEP06592, highly similar to AF151904 *H. sapiens* CGI-146 protein mRNA, mRNA sequence
208955_at	DUT	0.004075	810.9	3.18	dUTP pyrophosphatase
211519_s_at	KNSL6	0.004075	944.3	3.18	kinesin-like 6 (mitotic centromere-associated kinesin)

(continued on next page)

Table 2 (*continued*)

U133A probe set	Gene symbol	WRS *P* value	Average for CVX	Ratio CVX/NCK	Activity or Description
219258_at	FLJ20516	0.009023	511.3	3.18	hypothetical protein FLJ20516
212525_s_at	H2AFX	0.004075	405.9	3.15	H2A histone family, member X
1053_at	RFC2	0.009023	1062.0	3.13	replication factor C (activator 1) 2, 40 kDa
204689_at	HHEX	0.004075	182.8	3.07	hematopoietically expressed homeobox
202503_s_at	KIAA0101	0.004075	4870.9	3.07	KIAA0101 gene product
218979_at	FLJ12888	0.009023	495.9	3.07	hypothetical protein FLJ12888
204318_s_at	GTSE1	0.009023	536.4	3.06	G-2 and S-phase expressed 1
221677_s_at	DONSON	0.009023	605.2	3.06	downstream neighbor of SON
205356_at	USP13	0.004075	654.9	3.05	ubiquitin-specific protease 13 (isopeptidase T-3)
208694_at	PRKDC	0.006112	928.1	3.04	protein kinase, DNA-activated, catalytic polypeptide
206511_s_at	SIX2	0.009023	211.3	2.99	sine oculis homeobox homolog 2 (*Drosophila*)
205053_at	PRIM1	0.009023	1168.5	2.98	primase, polypeptide 1, 49 kDa
209053_s_at	WHSC1	0.009023	864.3	2.96	Wolf–Hirschhorn syndrome candidate 1
212279_at	MAC30	0.006112	2371.8	2.95	hypothetical protein MAC30
209408_at	KNSL6	0.004075	1835.2	2.94	kinesin-like 6 (mitotic centromere-associated kinesin)
203637_s_at	MID1	0.006112	441.3	2.93	midline 1 (Opitz/BBB syndrome)
205296_at	–	0.004075	74.2	2.92	
205519_at	FLJ12973	0.009023	280.3	2.91	hypothetical protein FLJ12973
214507_s_at	RRP4	0.006112	822.1	2.91	homolog of yeast RRP4 (ribosomal RNA processing 4), 3′-5′-exoribonuclease
204826_at	CCNF	0.004075	520.9	2.90	cyclin F
208447_s_at	PRPS1	0.006112	1244.9	2.88	phosphoribosyl pyrophosphate synthetase 1
202942_at	ETFB	0.004075	2047.6	2.84	electron-transfer-flavoprotein, beta polypeptide
212655_at	BDG-29	0.004075	312.9	2.83	BDG-29 protein
211717_at	MGC15396	0.004075	592.3	2.83	hypothetical protein MGC15396
209527_at	RRP4	0.006112	573.3	2.82	homolog of yeast RRP4 (ribosomal RNA processing 4), 3′-5′-exoribonuclease
222250_s_at	DKFZP434B168	0.004075	295.1	2.79	DKFZP434B168 protein
212349_at	POFUT1	0.004075	335.6	2.79	protein *O*-fucosyltransferase 1
218365_s_at	FLJ10514	0.009023	646.6	2.79	hypothetical protein FLJ10514
219061_s_at	DXS9879E	0.009023	1531.8	2.77	DNA segment on chromosome X (unique) 9879 expressed sequence
212379_at	GART	0.006112	1102.3	2.77	phosphoribosylglycineamide formyltransferase, phosphoribosylglycineamide synthetase, phosphoribosylaminoimidazole synthetase
211713_x_at	KIAA0101	0.009023	446.5	2.77	KIAA0101 gene product
203554_x_at	PTTG1	0.009023	6061.0	2.76	pituitary tumor-transforming 1
210216_x_at	RAD1	0.004075	1256.7	2.76	RAD1 homolog (*S. pombe*)
201043_s_at	ANP32A	0.006112	864.4	2.74	acidic (leucine-rich) nuclear phosphoprotein 32 family, member A
209832_s_at	CDT1	0.009023	558.2	2.72	DNA replication factor
209507_at	RPA3	0.004075	3086.1	2.71	replication protein A3, 14 kDa
222270_at	KIAA1387	0.004075	76.2	2.71	KIAA1387 protein
203660_s_at	PCNT2	0.004075	416.2	2.70	pericentrin 2 (kendrin)
200884_at	CKB	0.006112	1345.4	2.70	creatine kinase, brain
202309_at	MTHFD1	0.004075	2550.5	2.70	methylenetetrahydrofolate dehydrogenase (NADP + dependent), methylenetetrahydrofolate cyclohydrolase, formyltetrahydrofolate synthetase
208445_s_at	BAZ1B	0.009023	691.0	2.70	bromodomain adjacent to zinc finger domain, 1B
202602_s_at	HTATSF1	0.004075	643.1	2.69	HIV TAT-specific factor 1
202911_at	MSH6	0.009023	1609.6	2.69	mutS homolog 6 (*E. coli*)
39966_at	CSPG5	0.006112	178.1	2.69	chondroitin sulfate proteoglycan 5 (neuroglycan C)
210115_at	RPL39L	0.004075	1148.9	2.67	ribosomal protein L39-like
214035_x_at	NPIP	0.006112	1322.6	2.66	nuclear pore complex-interacting protein
205425_at	HIP1	0.009023	237.8	2.66	huntingtin-interacting protein 1
211080_s_at	NEK2	0.009023	302.3	2.65	NIMA (never in mitosis gene a)-related kinase 2
220011_at	MGC2603	0.009023	620.5	2.65	hypothetical protein MGC2603
2028_s_at	E2F1	0.009023	547.2	2.65	E2F transcription factor 1
216969_s_at	KNSL4	0.004075	413.3	2.64	kinesin-like 4
201697_s_at	DNMT1	0.009023	1883.1	2.64	DNA (cytosine-5-)-methyltransferase 1
204460_s_at	RAD1	0.004075	858.8	2.62	RAD1 homolog (*S. pombe*)
212483_at	IDN3	0.006112	216.4	2.61	IDN3 protein

Table 2 (*continued*)

U133A probe set	Gene symbol	WRS *P* value	Average for CVX	Ratio CVX/NCK	Activity or Description
214086_s_at	ADPRTL2	0.004075	626.6	2.59	ADP-ribosyltransferase (NAD+; poly(ADP-ribose) polymerase)-like 2
221311_x_at	DJ122O8.2	0.004075	300.2	2.58	hypothetical protein dJ122O8.2
211042_x_at	–	0.004075	993.6	2.55	similar to melanoma adhesion molecule (*H. sapiens*), mRNA sequence
209440_at	PRPS1	0.009023	1836.9	2.54	phosphoribosyl pyrophosphate synthetase 1
200875_s_at	NOL5A	0.009023	2193.3	2.53	nucleolar protein 5A (56 kDa with KKE/D repeat)
216299_s_at	XRCC3	0.009023	185.8	2.52	X-ray repair complementing defective repair in Chinese hamster cells 3
221952_x_at	KIAA1393	0.004075	7245.2	2.51	KIAA1393 protein
213378_s_at	DDX11	0.004075	979.4	2.51	DEAD/H (Asp-Glu-Ala-Asp/His) box polypeptide 11 (CHL1-like helicase homolog, *S. cerevisiae*)
203825_at	BRD3	0.004075	1424.2	2.50	bromodomain containing 3
222147_s_at	FLJ12785	0.004075	466.8	2.49	hypothetical protein FLJ12785
219004_s_at	C21orf45	0.009023	503.5	2.49	chromosome 21 open reading frame 45
201589_at	SMC1L1	0.009023	1778.6	2.49	SMC1 structural maintenance of chromosomes 1-like 1 (yeast)
206499_s_at	CHC1	0.006112	1665.1	2.47	chromosome condensation 1
218904_s_at	FLJ10110	0.004075	232.1	2.47	hypothetical protein FLJ10110
206261_at	ZNF239	0.009023	247.7	2.44	zinc finger protein 239
203564_at	FANCG	0.009023	1117.1	2.44	Fanconi anemia, complementation group G
202487_s_at	H2AV	0.004075	4737.6	2.43	histone H2A.F/Z variant
215708_s_at	PRIM2A	0.006112	368.5	2.42	primase, polypeptide 2A, 58 kDa
209932_s_at	DUT	0.009023	3621.3	2.42	dUTP pyrophosphatase
215722_s_at	SNRPA1	0.004075	579.1	2.41	small nuclear ribonucleoprotein polypeptide A′
204461_x_at	RAD1	0.006112	881.1	2.41	RAD1 homolog (*S. pombe*)
203022_at	RNASEH2A	0.009023	2305.8	2.41	ribonuclease H2, large subunit
204849_at	TCFL5	0.009023	889.5	2.40	transcription factor-like 5 (basic helix-loop-helix)
209520_s_at	NCBP1	0.009023	412.8	2.40	nuclear cap binding protein subunit 1, 80 kDa
37425_g_at	C6orf18	0.006112	326.1	2.40	chromosome 6 open reading frame 18
205339_at	SIL	0.009023	415.0	2.39	TAL1 (SCL) interrupting locus
221550_at	COX15	0.004075	207.8	2.38	COX15 homolog, cytochrome *c* oxidase assembly protein (yeast)
221556_at	CDC14B	0.009023	358.7	2.38	CDC14 cell division cycle 14 homolog B (*S. cerevisiae*)
203588_s_at	TFDP2	0.009023	795.2	2.38	transcription factor Dp-2 (E2F dimerization partner 2)
208985_s_at	EIF3S1	0.004075	1203.8	2.37	eukaryotic translation initiation factor 3, subunit 1 alpha, 35 kDa
210544_s_at	ALDH3A2	0.004075	791.2	2.36	aldehyde dehydrogenase 3 family, member A2
212330_at	TFDP1	0.006112	2623.8	2.35	transcription factor Dp-1
205176_s_at	ITGB3BP	0.006112	888.8	2.34	integrin beta 3 binding protein (beta3-endonexin)
208511_at	PTTG3	0.009023	310.4	2.32	pituitary tumor-transforming 3
203062_s_at	KIAA0170	0.004075	733.1	2.32	KIAA0170 gene product
204449_at	PDCL	0.009023	93.3	2.32	phosducin-like
217822_at	WBP11	0.009023	1584.7	2.32	WW domain binding protein 11
200956_s_at	SSRP1	0.004075	2249.4	2.32	structure-specific recognition protein 1
218440_at	MCCC1	0.006112	559.6	2.31	methylcrotonoyl-coenzyme A carboxylase 1 (alpha)
221931_s_at	SEC13L	0.009023	1053.9	2.30	sec13-like protein
204649_at	TROAP	0.004075	544.0	2.28	trophinin-associated protein (tastin)
215933_s_at	HHEX	0.009023	160.6	2.28	hematopoietically expressed homeobox
208939_at	SPS	0.006112	676.6	2.27	selenophosphate synthetase
212901_s_at	CSTF2T	0.009023	313.5	2.27	likely ortholog of mouse variant polyadenylation protein CSTF-64
213090_s_at	TAF4	0.004075	670.9	2.27	TAF4 RNA polymerase II, TATA box binding protein (TBP)-associated factor, 135 kDa
211040_x_at	GTSE1	0.004075	905.1	2.26	G-2 and S-phase expressed 1
209161_at	PRPF4	0.006112	2008.7	2.25	PRP4 pre-mRNA processing factor 4 homolog (yeast)
210625_s_at	AKAP1	0.006112	523.1	2.24	A kinase (PRKA) anchor protein 1
218269_at	RNASE3L	0.004075	1094.8	2.24	putative ribonuclease III
211318_s_at	RAE1	0.006112	2066.9	2.23	RAE1 RNA export 1 homolog (*S. pombe*)
212381_at	USP24	0.009023	195.1	2.22	ubiquitin-specific protease 24
208644_at	ADPRT	0.009023	1558.0	2.22	ADP-ribosyltransferase [NAD+; poly(ADP-ribose) polymerase]

(continued on next page)

Table 2 (*continued*)

U133A probe set	Gene symbol	WRS *P* value	Average for CVX	Ratio CVX/NCK	Activity or Description
209273_s_at	MGC4276	0.004075	824.0	2.21	hypothetical protein MGC4276 similar to CG8198
219531_at	FLJ10565	0.006112	486.4	2.21	hypothetical protein FLJ10565
209450_at	OSGEP	0.004075	438.0	2.20	*O*-sialoglycoprotein endopeptidase
202053_s_at	ALDH3A2	0.009023	2100.1	2.20	aldehyde dehydrogenase 3 family, member A2
212801_at	CIT	0.004075	860.0	2.20	citron (rho-interacting, serine/threonine kinase 21)
206055_s_at	SNRPA1	0.009023	1212.0	2.20	small nuclear ribonucleoprotein polypeptide A′
218653_at	SLC25A15	0.009023	662.0	2.19	solute carrier family 25 (mitochondrial carrier; ornithine transporter) member 15
207746_at	POLQ	0.006112	206.3	2.18	polymerase (DNA directed), theta
202726_at	LIG1	0.006112	577.9	2.18	ligase I, DNA, ATP-dependent
212287_at	JJAZ1	0.009023	836.4	2.17	joined to JAZF1
220773_s_at	GPHN	0.004075	361.1	2.17	gephyrin
218947_s_at	FLJ10486	0.006112	454.1	2.13	hypothetical protein FLJ10486
219875_s_at	PNAS-4	0.009023	111.1	2.12	CGI-146 protein
202622_s_at	SCA2	0.006112	507.3	2.12	spinocerebellar ataxia 2 (olivopontocerebellar ataxia 2, autosomal dominant, ataxin 2)
209162_s_at	PRPF4	0.004075	1404.4	2.12	PRP4 pre-mRNA processing factor 4 homolog (yeast)
218176_at	MAGEF1	0.009023	695.9	2.11	MAGEF1 protein
220094_s_at	FLJ20958	0.009023	1742.0	2.10	hypothetical protein FLJ20958
218229_s_at	POGK	0.006112	1467.9	2.09	pogo transposable element with KRAB domain
200975_at	PPT1	0.004075	2750.4	2.08	palmitoyl-protein thioesterase 1 (ceroid-lipofuscinosis, neuronal 1, infantile)
203721_s_at	CGI-48	0.009023	1447.4	2.08	CGI-48 protein
212170_at	RBM12	0.006112	168.9	2.06	RNA binding motif protein 12
221058_s_at	CKLF1	0.009023	732.4	2.06	chemokine-like factor 1
219161_s_at	CKLF1	0.004075	1185.7	2.06	chemokine-like factor 1
208956_x_at	DUT	0.004075	4399.2	2.04	dUTP pyrophosphatase
209433_s_at	PPAT	0.009023	361.7	2.04	phosphoribosyl pyrophosphate amidotransferase
201528_at	RPA1	0.009023	1958.2	2.03	replication protein A1, 70 kDa
201675_at	AKAP1	0.009023	1451.6	2.03	A kinase (PRKA) anchor protein 1
202466_at	POLS	0.006112	1679.5	2.02	polymerase (DNA directed) Sigma
203338_at	PPP2R5E	0.009023	719.0	2.02	protein phosphatase 2, regulatory subunit B (B56), epsilon isoform
201764_at	MGC5576	0.006112	2131.4	2.01	hypothetical protein MGC5576
204228_at	PPIH	0.004075	1605.2	2.01	peptidyl prolyl isomerase H (cyclophilin H)
219644_at	NY-REN-58	0.004075	96.8	2.01	NY-REN-58 antigen
218770_s_at	FLJ10315	0.004075	778.2	2.01	hypothetical protein FLJ10315
218586_at	C20orf20	0.004075	1017.5	2.01	chromosome 20 open reading frame 20

0.0109). Thus, q-RT-PCR data suggest that most array probe sets are likely to measure accurately the levels of the intended transcript within a complex mixture of transcripts.

CDKN2A/p16 expression by flow cytometry on primary CVX and NCK cell lines

An important issue is whether differences in gene expression result in meaningful differences in protein expression. Because the *CDKN2A* gene product, the p16 protein, has recently been explored as a potential diagnostic marker for cervical squamous and glandular neoplastic lesions as well as to identify individual dyskaryotic cells in Pap smears (Murphy et al., 2003), expression of p16 protein by flow cytometry was analyzed on all the 15 primary cell lines. As a positive control, the HPV18-positive HeLa cervical cancer cell line, which is known to overexpress p16, was also studied. As representatively shown in Fig. 3, high intracellular levels of p16 expression was found on all primary CVX cell lines tested (100% positive cells for all CVX), with mean fluorescence intensity (MFI) ranging from 116 to 280. As expected, HeLa cells expressed high levels of p16 by flow cytometry (data not shown). In contrast, primary NCK cell lines were all found negative for p16 expression ($P < 0.01$) (Fig. 3). These results show that high expression of the *p16* gene product at the RNA level by the CVX cell lines correlates tightly with high protein expression.

CDKN2A/p16 and PTGES expression by immunohistology on CVX and NCK tissue blocks

To determine whether the high expression of the *CDKN2A/p16* and *PTGES* genes detected by microarray and confirmed by q-RT-PCR in primary cervical cancer cell lines is the result of a selection of a subpopulation of cancer cells present in the original tumor, or whether in

Table 3
Up-regulated genes expressed at least twofold higher in NCK compared with CVX

U133A probe set	Gene symbol	WRS *P* value	Average for NCK	Ratio NCK/CVX	Activity or description
208539_x_at	SPRR2B	0.004075	8837.1	101.37	small proline-rich protein 2B
219554_at	RHCG	0.004075	2320.8	51.52	Rhesus blood group, C glycoprotein
205680_at	MMP10	0.004075	3399.3	48.22	matrix metalloproteinase 10 (stromelysin 2)
213796_at	(SPRK)	0.004075	5268.4	31.10	Small proline-rich protein SPRK (human, odontogenic keratocysts, mRNA partial, 317 nt), mRNA sequence
202917_s_at	S100A8	0.004075	10,169.9	27.80	S100 calcium binding protein A8 (calgranulin A)
220620_at	NICE-1	0.004075	2336.7	25.95	NICE-1 protein
214370_at	S100A8	0.004075	229.3	23.20	S100 calcium binding protein A8 (calgranulin A)
218312_s_at	FLJ12895	0.004075	613.6	21.94	hypothetical protein FLJ12895
206371_at	FOLR3	0.004075	1295.4	20.95	folate receptor 3 (gamma)
203562_at	FEZ1	0.004075	5812.2	19.39	fasciculation and elongation protein zeta 1 (zygin I)
204818_at	HSD17B2	0.006112	2237.0	18.86	hydroxysteroid (17-beta) dehydrogenase 2
221898_at	T1A-2	0.004075	565.1	18.80	lung type-I cell membrane-associated glycoprotein
205064_at	SPRR1B	0.004075	12,148.4	18.48	small proline-rich protein 1B (cornifin)
204475_at	MMP1	0.004075	7151.8	18.31	matrix metalloproteinase 1 (interstitial collagenase)
203691_at	PI3	0.004075	9690.8	18.26	protease inhibitor 3, skin-derived (SKALP)
220724_at	FLJ21511	0.004075	192.3	17.82	hypothetical protein FLJ21511
219630_at	DD96	0.004075	1999.5	16.94	epithelial protein up-regulated in carcinoma, membrane-associated protein 17
204463_s_at	EDNRA	0.004075	205.8	15.77	endothelin receptor type A
210065_s_at	UPK1B	0.004075	856.7	15.52	uroplakin 1B
209570_s_at	D4S234E	0.004075	264.4	14.90	DNA segment on chromosome 4 (unique) 234 expressed sequence
207526_s_at	IL1RL1	0.004075	1694.8	14.26	interleukin 1 receptor-like 1
214549_x_at	SPRR1A	0.004075	4380.8	13.57	small proline-rich protein 1A
202828_s_at	MMP14	0.004075	1264.2	12.81	matrix metalloproteinase 14 (membrane-inserted)
214702_at	FN1	0.004075	405.6	12.43	fibronectin 1
204470_at	CXCL1	0.006112	1774.5	12.13	chemokine (C-X-C motif) ligand 1 (melanoma growth stimulating activity, alpha)
211597_s_at	LAGY	0.004075	1096.1	11.78	homeodomain only protein
212657_s_at	IL1RN	0.004075	5546.0	11.66	interleukin 1 receptor antagonist
209278_s_at	TFPI2	0.009023	7097.0	11.53	tissue factor pathway inhibitor 2
220322_at	IL1F9	0.004075	713.0	11.06	interleukin 1 family, member 9
218990_s_at	SPRR3	0.004075	2080.6	10.99	small proline-rich protein 3
217109_at	MUC4	0.009023	293.6	10.97	mucin 4, tracheobronchial
219655_at	C7orf10	0.004075	1192.4	10.74	chromosome 7 open reading frame 10
209800_at	KRT16	0.009023	9227.6	10.58	keratin 16 (focal nonepidermolytic palmoplantar keratoderma)
205899_at	CCNA1	0.009023	1237.4	9.61	cyclin A1
219993_at	SOX17	0.004075	786.6	9.56	SRY (sex determining region Y)-box 17
41469_at	(PI3?)	0.004075	7523.9	9.40	
205479_s_at	PLAU	0.004075	8178.8	9.35	plasminogen activator, urokinase
213680_at	KRT6B	0.006112	9562.0	9.03	keratin 6B
201667_at	GJA1	0.006112	1507.4	8.97	gap junction protein, alpha 1, 43 kDa (connexin 43)
204464_s_at	EDNRA	0.004075	690.9	8.81	endothelin receptor type A
205778_at	KLK7	0.004075	3534.8	8.79	kallikrein 7 (chymotryptic, stratum corneum)
211756_at	PTHLH	0.009023	2389.2	8.78	parathyroid hormone-like hormone
211668_s_at	PLAU	0.004075	8066.0	8.51	plasminogen activator, urokinase
222020_s_at	HNT	0.004075	231.3	8.37	neurotrimin
216243_s_at	IL1RN	0.006112	3602.1	8.29	interleukin 1 receptor antagonist
202859_x_at	IL8	0.006112	3803.8	8.18	interleukin 8
212659_s_at	IL1RN	0.004075	2445.9	8.16	interleukin 1 receptor antagonist
209949_at	NCF2	0.004075	1197.1	8.15	neutrophil cytosolic factor 2 (65 kDa, chronic granulomatous disease, autosomal 2)
209569_x_at	D4S234E	0.004075	1014.5	7.99	DNA segment on chromosome 4 (unique) 234 expressed sequence
210355_at	PTHLH	0.004075	1802.2	7.69	parathyroid hormone-like hormone
214701_s_at	FN1	0.004075	4124.9	7.69	fibronectin 1
207850_at	CXCL3	0.009023	640.5	7.66	chemokine (C-X-C motif) ligand 3
220723_s_at	FLJ21511	0.004075	315.8	7.63	hypothetical protein FLJ21511

(continued on next page)

Table 3 (*continued*)

U133A probe set	Gene symbol	WRS *P* value	Average for NCK	Ratio NCK/CVX	Activity or description
213524_s_at	G0S2	0.009023	7490.5	7.54	putative lymphocyte G0/G1 switch gene
201859_at	PRG1	0.009023	2434.6	7.51	proteoglycan 1, secretory granule
212531_at	LCN2	0.006112	11,606.6	7.42	lipocalin 2 (oncogene 24p3)
202283_at	SERPINF1	0.004075	486.2	7.40	serine (or cysteine) proteinase inhibitor, clade F (alpha-2 antiplasmin, pigment epithelium-derived factor), member 1
203423_at	RBP1	0.004075	2062.5	7.35	retinol binding protein 1, cellular
211506_s_at	IL8	0.006112	1262.9	7.26	interleukin 8
206153_at	CYP4F11	0.004075	429.6	7.12	cytochrome P450, subfamily IVF, polypeptide 11
38037_at	DTR	0.009023	2554.9	7.10	diphtheria toxin receptor (heparin-binding epidermal growth factor-like growth factor)
209182_s_at	DEPP	0.004075	579.9	6.93	decidual protein induced by progesterone
208607_s_at	SAA2	0.006112	1443.9	6.92	serum amyloid A2
204614_at	SERPINB2	0.004075	5055.3	6.81	serine (or cysteine) proteinase inhibitor, clade B (ovalbumin), member 2
212646_at	KIAA0084	0.004075	1195.6	6.76	KIAA0084 protein
206191_at	ENTPD3	0.004075	1342.7	6.69	ectonucleoside triphosphate diphosphohydrolase 3
206421_s_at	SERPINB7	0.004075	1235.3	6.63	serine (or cysteine) proteinase inhibitor, clade B (ovalbumin), member 7
206453_s_at	NDRG2	0.004075	1865.9	6.50	NDRG family member 2
209550_at	NDN	0.004075	1108.7	6.49	necdin homolog (mouse)
216244_at	IL1RN	0.004075	214.6	6.41	interleukin 1 receptor antagonist
203726_s_at	LAMA3	0.006112	10,518.0	6.34	laminin, alpha 3
210064_s_at	UPK1B	0.004075	1029.1	6.19	uroplakin 1B
218963_s_at	HAIK1	0.009023	3314.0	6.12	type I intermediate filament cytokeratin
205403_at	IL1R2	0.009023	279.0	6.07	interleukin 1 receptor, type II
206467_x_at	TNFRSF6B	0.004075	2452.8	6.06	tumor necrosis factor receptor superfamily, member 6b, decoy
210118_s_at	IL1A	0.004075	3930.9	5.87	interleukin 1, alpha
209546_s_at	APOL1	0.009023	933.3	5.84	apolipoprotein L, 1
39402_at	IL1B	0.004075	5315.9	5.72	interleukin 1, beta
203535_at	S100A9	0.004075	8545.5	5.68	S100 calcium binding protein A9 (calgranulin B)
206662_at	GLRX	0.004075	3109.1	5.61	glutaredoxin (thioltransferase)
214841_at	FLJ38993	0.009023	260.9	5.46	hypothetical protein FLJ38993
209552_at	PAX8	0.009023	477.2	5.44	paired box gene 8
220230_s_at	CYB5R2	0.004075	1110.9	5.42	cytochrome b5 reductase b5R.2
206857_s_at	FKBP1B	0.004075	1630.9	5.36	FK506 binding protein 1B, 12.6 kDa
204105_s_at	NRCAM	0.004075	541.4	5.34	neuronal cell adhesion molecule
205067_at	IL1B	0.006112	8008.3	5.31	interleukin 1, beta
209159_s_at	NDRG4	0.004075	633.9	5.29	NDRG family member 4
219412_at	RAB38	0.009023	3944.4	5.26	RAB38, member RAS oncogene family
209772_s_at	CD24	0.004075	3481.1	5.25	CD24 antigen (small cell lung carcinoma cluster 4 antigen)
202267_at	LAMC2	0.004075	13,582.0	5.11	laminin, gamma 2
218960_at	TMPRSS4	0.009023	1622.0	4.97	transmembrane protease, serine 4
209652_s_at	PGF	0.004075	816.1	4.96	placental growth factor, vascular endothelial growth factor-related protein
200953_s_at	CCND2	0.009023	4301.1	4.93	cyclin D2
204249_s_at	LMO2	0.004075	357.9	4.78	LIM domain only 2 (rhombotin-like 1)
203234_at	UP	0.006112	8821.8	4.75	uridine phosphorylase
212464_s_at	FN1	0.004075	15,099.1	4.73	fibronectin 1
207571_x_at	ICB-1	0.004075	647.9	4.69	basement membrane-induced gene
203037_s_at	KIAA0429	0.004075	2081.5	4.69	KIAA0429 gene product
219697_at	HS3ST2	0.004075	816.2	4.65	heparan sulfate (glucosamine) 3-*O*-sulfotransferase 2
204469_at	PTPRZ1	0.004075	204.3	4.58	protein tyrosine phosphatase, receptor-type, Z polypeptide 1
206893_at	SALL1	0.009023	158.6	4.55	sal-like 1 (*Drosophila*)
204726_at	CDH13	0.004075	404.2	4.47	cadherin 13, H-cadherin (heart)
211719_x_at	FN1	0.004075	15,762.8	4.45	fibronectin 1
205349_at	GNA15	0.006112	2220.4	4.43	guanine nucleotide binding protein (G protein), alpha 15 (Gq class)
210248_at	WNT7A	0.009023	1468.9	4.41	wingless-type MMTV integration site family, member 7A

Table 3 (*continued*)

U133A probe set	Gene symbol	WRS *P* value	Average for NCK	Ratio NCK/CVX	Activity or description
205404_at	HSD11B1	0.006112	474.5	4.39	hydroxysteroid (11-beta) dehydrogenase 1
206042_x_at	SNURF	0.004075	2260.1	4.39	SNRPN upstream reading frame
210785_s_at	ICB-1	0.004075	717.2	4.32	basement membrane-induced gene
204971_at	CSTA	0.004075	9892.5	4.32	cystatin A (stefin A)
217983_s_at	RNASE6PL	0.004075	5008.8	4.28	ribonuclease 6 precursor
207675_x_at	ARTN	0.006112	1546.9	4.28	artemin
214175_x_at	RIL	0.004075	1563.6	4.28	LIM domain protein
206584_at	MD-2	0.006112	236.6	4.26	MD-2 protein
204542_at	STHM	0.009023	2367.7	4.24	sialyltransferase
202957_at	HCLS1	0.004075	684.2	4.16	hematopoietic cell-specific Lyn substrate 1
216052_x_at	ARTN	0.004075	1361.0	4.15	artemin
209487_at	RBPMS	0.006112	1455.5	4.12	RNA-binding protein gene with multiple splicing
202157_s_at	CUGBP2	0.006112	559.8	4.06	CUG triplet repeat, RNA binding protein 2
209348_s_at	MAF	0.006112	253.0	4.02	v-maf musculoaponeurotic fibrosarcoma oncogene homolog (avian)
206714_at	ALOX15B	0.004075	672.9	3.99	arachidonate 15-lipoxygenase, second type
221854_at	(Plakophilin-1-like)	0.009023	2825.0	3.93	ESTs, highly similar to plakophilin 1; Plakophilin-1 (*H. sapiens*)
209270_at	LAMB3	0.004075	15,685.9	3.92	laminin, beta 3
213275_x_at	CTSB	0.006112	3187.9	3.92	cathepsin B
219995_s_at	FLJ13841	0.004075	345.5	3.89	hypothetical protein FLJ13841
218694_at	ALEX1	0.006112	308.8	3.86	ALEX1 protein
209822_s_at	VLDLR	0.004075	620.8	3.80	very low density lipoprotein receptor
208650_s_at	CD24	0.004075	3639.2	3.80	CD24 antigen (small cell lung carcinoma cluster 4 antigen)
202948_at	IL1R1	0.004075	357.3	3.75	interleukin 1 receptor, type I
203722_at	ALDH4A1	0.006112	522.2	3.71	aldehyde dehydrogenase 4 family, member A1
212647_at	RRAS	0.004075	3810.4	3.66	related RAS viral (r-ras) oncogene homolog
203085_s_at	TGFB1	0.004075	2186.8	3.66	transforming growth factor, beta 1 (Camurati–Engelmann disease)
203256_at	CDH3	0.006112	8511.9	3.63	cadherin 3, type 1, P-cadherin (placental)
209488_s_at	RBPMS	0.009023	1336.4	3.60	RNA-binding protein gene with multiple splicing
204636_at	COL17A1	0.004075	3217.5	3.60	collagen, type XVII, alpha 1
217279_x_at	MMP14	0.004075	1101.3	3.60	matrix metalloproteinase 14 (membrane-inserted)
203180_at	ALDH1A3	0.006112	8439.8	3.58	aldehyde dehydrogenase 1 family, member A3
204952_at	C4.4A	0.006112	2024.0	3.51	GPI-anchored metastasis-associated protein homolog
210105_s_at	FYN	0.006112	1251.1	3.50	FYN oncogene related to SRC, FGR, YES
204205_at	APOBEC3G	0.009023	601.8	3.46	apolipoprotein B mRNA editing enzyme, catalytic polypeptide-like 3G
212509_s_at	(EST)	0.004075	7133.5	3.45	ESTs, weakly similar to hypothetical protein FLJ22184 (*H. sapiens*)
219257_s_at	SPHK1	0.004075	2472.3	3.43	sphingosine kinase 1
209356_x_at	EFEMP2	0.009023	350.2	3.41	EGF-containing fibulin-like extracellular matrix protein 2
213572_s_at	SERPINB1	0.009023	1735.9	3.40	serine (or cysteine) proteinase inhibitor, clade B (ovalbumin), member 1
266_s_at	CD24	0.004075	2423.9	3.37	CD24 antigen (small cell lung carcinoma cluster 4 antigen)
213533_at	D4S234E	0.004075	363.9	3.34	DNA segment on chromosome 4 (unique) 234 expressed sequence
211317_s_at	CFLAR	0.009023	575.3	3.33	CASP8 and FADD-like apoptosis regulator
217730_at	PP1201	0.006112	5059.5	3.32	PP1201 protein
219681_s_at	RCP	0.004075	1499.8	3.32	Rab coupling protein
221666_s_at	ASC	0.006112	2377.4	3.28	apoptosis-associated speck-like protein containing a CARD
210495_x_at	FN1	0.004075	16,981.8	3.28	fibronectin 1
205011_at	LOH11CR2A	0.004075	850.1	3.24	loss of heterozygosity, 11, chromosomal region 2, gene A
214279_s_at	NDRG2	0.006112	642.7	3.22	NDRG family member 2
218319_at	PELI1	0.004075	368.9	3.21	pellino homolog 1 (*Drosophila*)
203817_at	GUCY1B3	0.004075	182.1	3.20	guanylate cyclase 1, soluble, beta 3
201645_at	TNC	0.004075	1481.5	3.16	tenascin C (hexabrachion)

(continued on next page)

Table 3 (*continued*)

U133A probe set	Gene symbol	WRS *P* value	Average for NCK	Ratio NCK/CVX	Activity or description
202644_s_at	TNFAIP3	0.006112	2418.5	3.16	tumor necrosis factor, alpha-induced protein 3
209771_x_at	CD24	0.004075	11,152.3	3.15	CD24 antigen (small cell lung carcinoma cluster 4 antigen)
201522_x_at	SNRPN	0.004075	4769.3	3.12	small nuclear ribonucleoprotein polypeptide N
210163_at	CXCL11	0.009023	109.2	3.11	chemokine (C-X-C motif) ligand 11
200952_s_at	CCND2	0.009023	480.1	3.09	cyclin D2
209276_s_at	GLRX	0.006112	1825.8	3.09	glutaredoxin (thioltransferase)
212364_at	MYO1B	0.004075	1761.4	3.09	myosin IB
202181_at	KIAA0247	0.004075	1674.4	3.07	KIAA0247 gene product
216442_x_at	FN1	0.004075	17,126.0	3.07	fibronectin 1
211564_s_at	RIL	0.009023	1026.5	3.06	LIM domain protein
207836_s_at	RBPMS	0.009023	584.8	3.00	RNA-binding protein gene with multiple splicing
201508_at	IGFBP4	0.009023	1663.9	3.00	insulin-like growth factor binding protein 4
216379_x_at	CD24	0.006112	11,988.5	2.99	CD24 antigen (small cell lung carcinoma cluster 4 antigen)
213293_s_at	TRIM22	0.009023	1349.5	2.97	tripartite motif-containing 22
201286_at	(SDC1)	0.004075	6578.9	2.97	
204638_at	ACP5	0.009023	462.8	2.95	acid phosphatase 5, tartrate resistant
218840_s_at	FLJ10631	0.009023	514.0	2.94	hypothetical protein FLJ10631
219850_s_at	EHF	0.009023	425.3	2.93	ets homologous factor
219305_x_at	FBXO2	0.006112	1161.9	2.92	F-box only protein 2
214995_s_at	KA6	0.004075	495.5	2.91	induced upon T cell activation
202597_at	(EST)	0.006112	5474.0	2.89	ESTs, weakly similar to YYY1_HUMAN Very very hypothetical protein RMSA-1 (*H. sapiens*)
213988_s_at	SAT	0.004075	6926.0	2.86	spermidine/spermine N1-acetyltransferase
217930_s_at	TOLLIP	0.009023	1096.4	2.83	Toll-interacting protein
200986_at	SERPING1	0.009023	403.7	2.82	serine (or cysteine) proteinase inhibitor, clade G (C1 inhibitor), member 1, (angioedema, hereditary)
213272_s_at	LOC57146	0.006112	1178.8	2.82	hypothetical protein from clone 24796
200838_at	CTSB	0.004075	7430.5	2.80	cathepsin B
219476_at	MGC4309	0.004075	1859.1	2.75	hypothetical protein MGC4309
217118_s_at	KIAA0930	0.006112	2771.4	2.74	KIAA0930 protein
210001_s_at	SOCS1	0.009023	226.8	2.74	suppressor of cytokine signaling 1
204034_at	YF13H12	0.004075	7500.9	2.73	protein expressed in thyroid
210397_at	DEFB1	0.004075	267.1	2.71	defensin, beta 1
214580_x_at	KRT6A	0.009023	9411.7	2.71	keratin 6A
205676_at	CYP27B1	0.009023	636.9	2.71	cytochrome P450, subfamily XXVIIB (25-hydroxyvitamin D-1-alpha-hydroxylase), polypeptide 1
211862_x_at	CFLAR	0.006112	922.0	2.70	CASP8 and FADD-like apoptosis regulator
209126_x_at	KRT6B	0.009023	18,599.2	2.69	keratin 6B
200839_s_at	CTSB	0.004075	11,534.5	2.63	cathepsin B
160020_at	MMP14	0.004075	2631.4	2.60	matrix metalloproteinase 14 (membrane-inserted)
204682_at	LTBP2	0.006112	1541.7	2.59	latent transforming growth factor beta binding protein 2
207196_s_at	TNIP1	0.004075	3240.6	2.59	TNFAIP3-interacting protein 1
201631_s_at	IER3	0.004075	15,995.3	2.59	immediate early response 3
202074_s_at	OPTN	0.004075	1625.1	2.59	optineurin
202073_at	OPTN	0.004075	343.1	2.58	optineurin
208651_x_at	CD24	0.004075	3203.7	2.58	CD24 antigen (small cell lung carcinoma cluster 4 antigen)
205016_at	TGFA	0.004075	2539.3	2.58	transforming growth factor, alpha
212484_at	MTVR1	0.004075	1034.8	2.58	mouse mammary tumor virus receptor homolog 1
211552_s_at	ALDH4A1	0.006112	690.4	2.57	aldehyde dehydrogenase 4 family, member A1
213924_at	MPPE1	0.009023	404.2	2.55	metallophosphoesterase
209723_at	SERPINB9	0.009023	655.2	2.54	serine (or cysteine) proteinase inhibitor, clade B (ovalbumin), member 9
209030_s_at	IGSF4	0.004075	273.5	2.53	immunoglobulin superfamily, member 4
37408_at	MRC2	0.006112	1120.2	2.53	mannose receptor, C type 2
202643_s_at	TNFAIP3	0.006112	934.2	2.52	tumor necrosis factor, alpha-induced protein 3
211031_s_at	CYLN2	0.004075	431.3	2.52	cytoplasmic linker 2
209079_x_at	PCDHGA1	0.006112	2505.0	2.48	protocadherin gamma subfamily A, 1

Table 3 (*continued*)

U133A probe set	Gene symbol	WRS *P* value	Average for NCK	Ratio NCK/CVX	Activity or description
211654_x_at	HLA-DQB1	0.009023	478.3	2.47	major histocompatibility complex, class II, DQ beta 1
218531_at	FLJ21749	0.006112	1382.9	2.45	hypothetical protein FLJ21749
209369_at	ANXA3	0.009023	2942.1	2.44	annexin A3
218451_at	CDCP1	0.006112	2332.9	2.43	CUB domain-containing protein 1
40016_g_at	KIAA0303	0.004075	798.8	2.43	KIAA0303 protein
211066_x_at	PCDHGC3	0.006112	2531.6	2.41	protocadherin gamma subfamily C, 3
205789_at	CD1D	0.004075	159.7	2.40	CD1D antigen, d-polypeptide
214632_at	NRP2	0.004075	211.7	2.38	neurophilin 2
211824_x_at	DEFCAP	0.009023	155.8	2.38	death effector filament-forming Ced-4-like apoptosis protein
209508_x_at	CFLAR	0.004075	538.9	2.36	CASP8 and FADD-like apoptosis regulator
205375_at	MDFI	0.009023	775.8	2.36	MyoD family inhibitor
205180_s_at	ADAM8	0.006112	637.6	2.36	a disintegrin and metalloproteinase domain 8
209637_s_at	RGS12	0.006112	738.0	2.33	regulator of G-protein signaling 12
217858_s_at	ALEX3	0.006112	388.8	2.32	ALEX3 protein
38149_at	KIAA0053	0.009023	264.2	2.32	KIAA0053 gene product
220054_at	IL23A	0.004075	376.0	2.31	interleukin 23, alpha subunit p19
221756_at	MGC17330	0.004075	479.7	2.31	hypothetical protein MGC17330
220753_s_at	CRYL1	0.009023	871.3	2.30	crystallin, lambda 1
635_s_at	PPP2R5B	0.004075	513.4	2.28	protein phosphatase 2, regulatory subunit B (B56), beta isoform
205717_x_at	PCDHGC3	0.004075	1726.8	2.28	protocadherin gamma subfamily C, 3
201249_at	SLC2A1	0.004075	331.5	2.27	solute carrier family 2 (facilitated glucose transporter), member 1
204620_s_at	CSPG2	0.009023	239.3	2.27	chondroitin sulfate proteoglycan 2 (versican)
206355_at	GNAL	0.006112	152.8	2.26	guanine nucleotide binding protein (G protein), alpha activating activity polypeptide, olfactory type
211316_x_at	CFLAR	0.006112	995.8	2.26	CASP8 and FADD-like apoptosis regulator
201287_s_at	SDC1	0.004075	10,943.8	2.26	syndecan 1
64486_at	CORO1B	0.004075	2661.1	2.26	coronin, actin-binding protein, 1B
221757_at	MGC17330	0.004075	740.2	2.25	hypothetical protein MGC17330
209260_at	SFN	0.006112	10,326.6	2.23	stratifin
212736_at	BC008967	0.009023	260.1	2.23	hypothetical gene BC008967
205973_at	FEZ1	0.004075	259.5	2.22	fasciculation and elongation protein zeta 1 (zygin I)
202744_at	SLC20A2	0.009023	733.0	2.22	solute carrier family 20 (phosphate transporter), member 2
219267_at	GLTP	0.006112	1013.0	2.21	glycolipid transfer protein
203504_s_at	ABCA1	0.009023	464.4	2.21	ATP-binding cassette, subfamily A (ABC1), member 1
212956_at	KIAA0882	0.004075	492.0	2.19	KIAA0882 protein
214435_x_at	RALA	0.006112	1224.3	2.19	v-ral simian leukemia viral oncogene homolog A (ras related)
217867_x_at	BACE2	0.004075	2377.9	2.16	beta-site APP-cleaving enzyme 2
204447_at	ProSAPiP1	0.009023	429.0	2.15	ProSAPiP1 protein
215411_s_at	C6orf4	0.009023	1881.8	2.14	chromosome 6 open reading frame 4
204137_at	TM7SF1	0.006112	285.9	2.13	transmembrane 7 superfamily member 1 (up-regulated in kidney)
121_at	PAX8	0.009023	2773.5	2.13	paired box gene 8
206197_at	NME5	0.004075	192.2	2.12	nonmetastatic cells 5, protein expressed in (nucleoside-diphosphate kinase)
219489_s_at	RHBDL2	0.009023	5239.4	2.10	rhomboid, veinlet-like 2 (*Drosophila*)
208816_x_at	ANXA2P2	0.004075	6962.6	2.10	annexin A2 pseudogene 2
219368_at	NAP1L2	0.009023	64.5	2.07	nucleosome assembly protein 1-like 2
206581_at	BNC	0.006112	549.1	2.07	basonuclin
203725_at	GADD45A	0.004075	4735.3	2.07	growth arrest and DNA-damage-inducible, alpha
209912_s_at	KIAA0415	0.006112	203.7	2.07	KIAA0415 gene product
216383_at	-	0.009023	1036.4	2.07	
204334_at	KLF7	0.009023	671.2	2.06	Kruppel-like factor 7 (ubiquitous)
209931_s_at	FKBP1B	0.009023	356.2	2.06	FK506 binding protein 1B, 12.6 kDa
204319_s_at	RGS10	0.004075	1327.2	2.05	regulator of G-protein signaling 10
219202_at	FLJ22341	0.009023	693.4	2.04	hypothetical protein FLJ22341

(continued on next page)

Table 3 (*continued*)

U133A probe set	Gene symbol	WRS *P* value	Average for NCK	Ratio NCK/CVX	Activity or description
217971_at	MAP2K1IP1	0.004075	928.0	2.03	mitogen-activated protein kinase kinase 1-interacting protein 1
203686_at	MPG	0.009023	1145.1	2.03	*N*-methylpurine-DNA glycosylase
37152_at	PPARD	0.006112	1428.0	2.02	peroxisome proliferative activated receptor, delta
214104_at	(FLJ34550)	0.009023	327.4	2.02	*H. sapiens* cDNA FLJ34550 fis, clone HLUNG2009303, mRNA sequence
202180_s_at	MVP	0.004075	1852.8	2.00	major vault protein

vitro expansion conditions may have modified gene expression, we performed immunohistochemical analysis of CDKN2A/p16 and PTGES protein expression on formalin-fixed tissue from all uncultured primary surgical specimens of CVX and NCK tested in the gene expression analysis (Table 4). As representatively shown in Fig. 4, heavy nuclear and cytoplasmic staining for p16 protein expression was noted in all squamous, adenosqu-

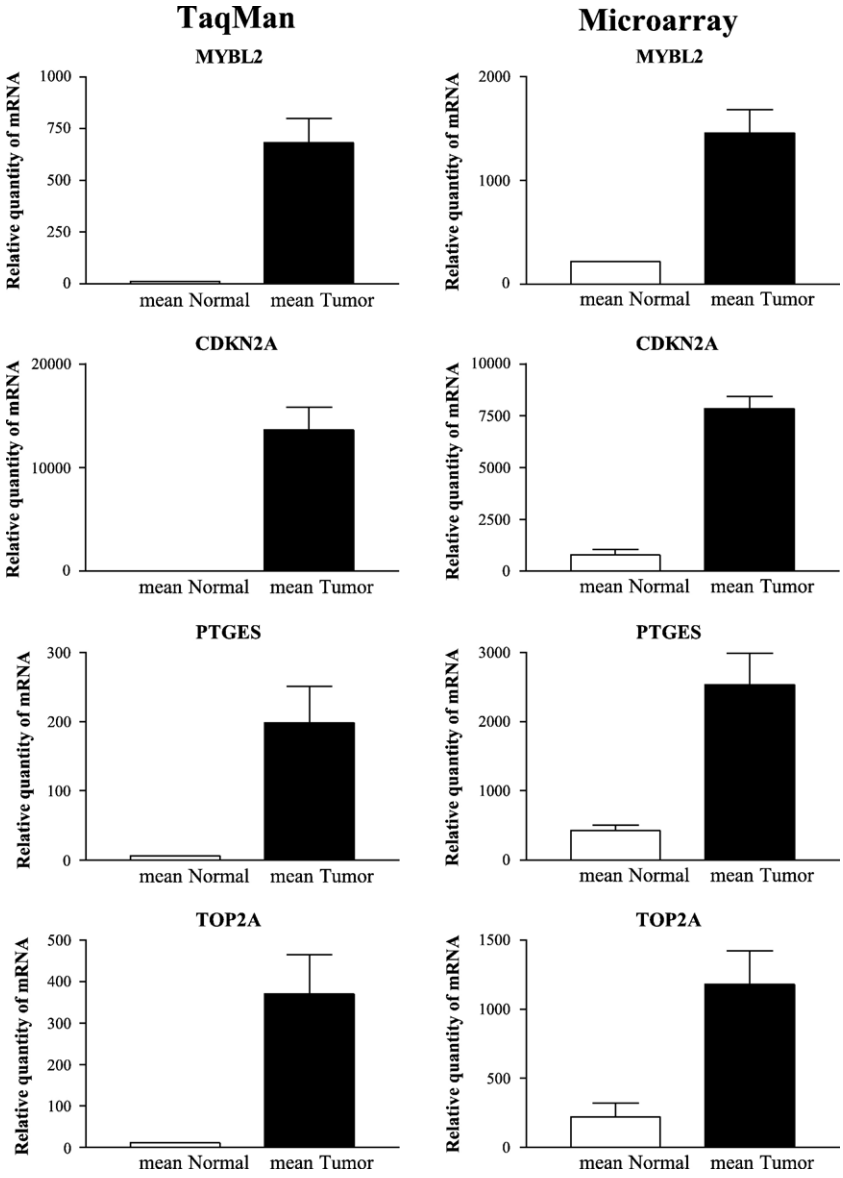

Fig. 2. Quantitative RT-PCR and microarray expression analysis of *CDKN2A*, *v-Myb*, *PTGES*, and *TOP2A* genes differentially expressed between CVX and NCK. qRT-PCR samples were run in duplicate. The results of one experiment are shown and are representative of two separate studies with similar results.

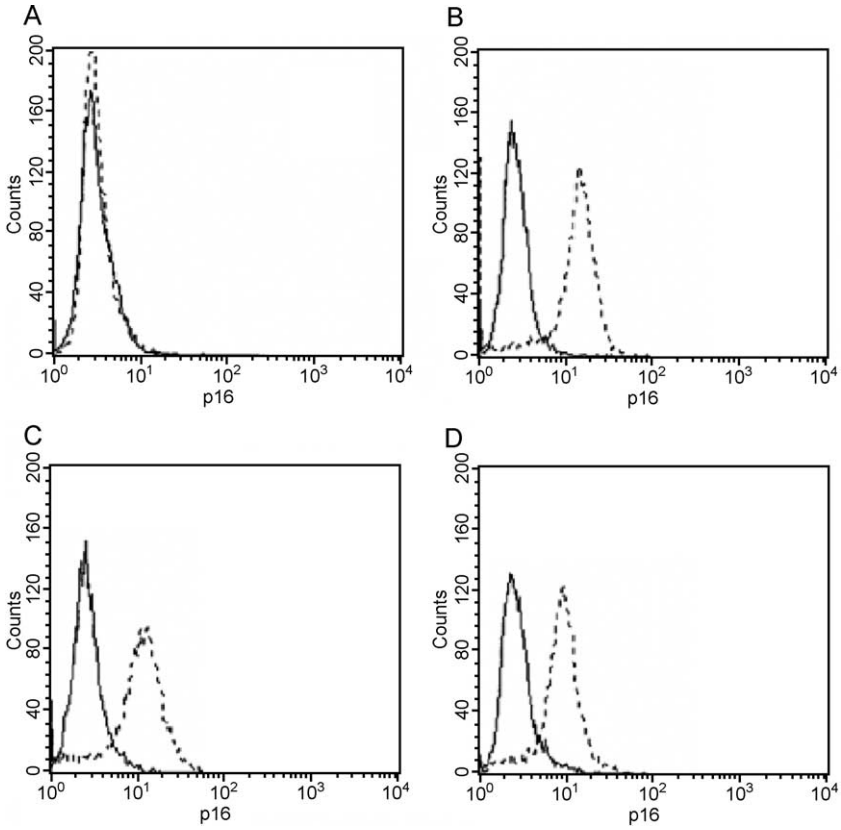

Fig. 3. Flow cytometric analysis of *CDKN2A/p16* staining of CVX primary and NCK cell lines. Representative histograms show *CDKN2A/p16* data in dashed lines while isotype control MAb profiles are shown in solid lines. NCK (A) showed negative staining for *CDKN2A/p16* while CVX 1 (B; squamous cervical cancer), CVX 2 (C; adenosquamous cervical cancer), and CVX 7 (D; adenocarcinoma) all showed strong positivity for *CDKN2A/p16* ($P < 0.01$ by Student's *t* test).

amous, and adenocarcinoma specimens that overexpressed the *CDKN2A* gene and its gene product by microarray and flow cytometry, respectively. In contrast, negative (i.e., score 0) staining was found in all NCK samples tested by immunohistochemistry (Table 4 and Fig. 4). As presented in Table 4 and representatively shown in Fig. 5, similar results were obtained when immunohistochemistry was carried out to demonstrate PTGES expression on tumor cells. Furthermore, focal intense or diffuse intense staining for CDKN2A/p16 and PTGES protein expression (i.e., score 2+ and 3+) was noted in the majority of the separate set of archival CVX specimens use for comparison (CVX-12 to CVX-22, Table 4). Thus, these data generated on an independent set of invasive cervical cancer specimens confirmed p16 and PTGES protein expression as two consistently positive markers to identify HPV-infected cervical cancer cells.

Discussion

The management of disseminated carcinoma of the cervix no longer amenable to control with surgery or radiation therapy has not improved significantly with modern chemotherapy; the 1-year survival among patients with such refractory disease remains at a dismal 10–15%. A deeper molecular understanding of host interactions with cervical carcinogenic factors and novel therapeutic strategies effective to prevent disease progression following first-line treatment remain desperately needed.

Large-scale gene expression analysis such as high-density oligonucleotide and cDNA microarrays represents a powerful new tool that has the potential to identify a number of differentially expressed genes in HPV-infected cervical cancers compared to normal cervical keratinocytes. These analyses may therefore lay the groundwork for future studies testing some of these markers for clinical utility in the diagnosis and eventually the treatment of this disease. This report represents the first communication of an investigation involving the genome-wide examination of differences in gene expression between primary HPV16 and HPV18-infected CVX and normal cervical epithelial cells (NCK). In this regard, although the possible changes in gene expression related to the removal of normal and cervical cancer cells from their microenvironment remains unknown, in this study we have used short-term primary CVX and NCK cultures (to minimize the risk of a selection bias inherent in any long-term in vitro growth) to study differential gene expression in highly enriched and homogeneous populations of cervical epithelial cells. In this work, cancer

Table 4
p16 and PTGES immunostaining in normal cervix keratinocytes and cancer

Case	Histology	p16/CDKN2A	PTGES
NCK-1	Squamous	–	–
NCK-2	Squamous	–	–
NCK-3	Squamous	–	–
NCK-4	Squamous	–	–
CVX-1	Squamous	++	+++
CVX-2	Adenosquamous	++	++
CVX-3	Squamous	++	++
CVX-4	Squamous	++	+++
CVX-5	Squamous	++	++
CVX-6	Squamous	++	++
CVX-7	Adenocarcinoma	++	+++
CVX-8	Adenocarcinoma	++	++
CVX-9	Adenosquamous	++	+
CVX-10	Adenosquamous	++	++
CVX-11	Adenocarcinoma	++	++
CVX-12	Squamous	++	++
CVX-13	Adenosquamous	++	++
CVX-14	Squamous	++	++
CVX-15	Squamous	++	+
CVX-16	Adenocarcinoma	++	++
CVX-17	Adenosquamous	+	+
CVX-18	Squamous	++	++
CVX-19	Squamous	++	+
CVX-20	Squamous	++	+++
CVX-21	Squamous	++	++
CVX-22	Squamous	++	++

cells derived from early stages invasive squamous, adenosquamous, and adenocarcinoma cervical tumors, which represent all the common histological types of cervical cancer, were included in the gene expression analysis.

We found that hierarchical clustering of the samples and gene expression levels within the samples led to the unambiguous separation of CVX and NCK. Of 1354 genes showing greater than twofold up- and down-regulation and a majority of detection = present calls in more than half of the samples, we identified 505 genes that were statistically significant by the WRS test at alpha = 0.01, with a one-sided upper 99% confidence limit of 20.48 false discoveries (4.05%). Of the 505 genes with WRS $P < 0.01$, 240 exhibited up-regulation and 265 exhibited down-regulation in CVX compared to NCK. The known function of some of these genes may provide insights in the biology of cervical tumors while others may prove to be useful diagnostic and therapeutic markers against CVX.

For example, the expression of genes required for progression through the cell cycle is highly modulated through a regulatory axis containing the E2F transcription factor and retinoblastoma (pRb) tumor suppressor protein families. Of interest, the cyclin-dependent kinase inhibitor 2A (*CDKN2A*) gene was found to be one of the most highly differentially expressed genes in CVX, with over 10-fold up-regulation relative to NCK. Importantly, *CDKN2A* gene is a putative oncosuppressor gene encoding two unrelated proteins, both cellular growth inhibitors, in different reading frames (Quelle et al., 1995; Sano et al., 2002). One is p16, which regulates retinoblastoma protein (pRb)-dependent G1 arrest; and the second is p14ARF, which blocks MDM2-induced p53 degradation resulting in an increase in p53 levels that leads to cell cycle arrest (Quelle et al., 1995; Sano et al., 2002). Because high-risk HPV E6 and E7 transforming oncoproteins are able to inactivate p53 and Rb tumor suppressor function, the marked overexpression of the *CDKN2A* gene may likely be a negative feedback phenomenon resulting from the functional inactivation of

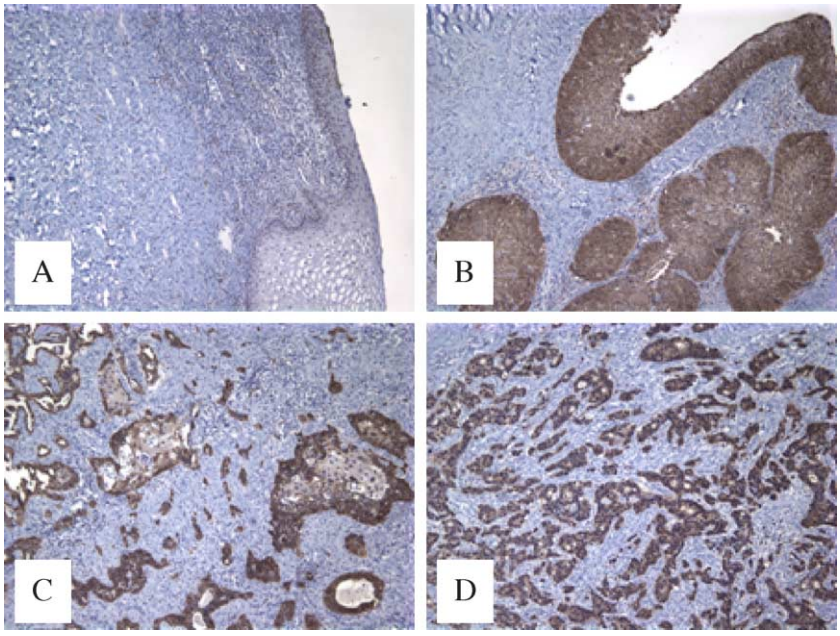

Fig. 4. Representative immunohistochemical staining for *CDKN2A/p16* markers of three paraffin-embedded CVX specimens and one NCK specimen. NCK (A) showed negative staining for *CDKN2A/p16* while CVX 1 (B; squamous cervical cancer), CVX 2 (C; adenosquamous cervical cancer), and CVX 7 (D; adenocarcinoma) showed diffuse staining for *CDKN2A/p16*. Original magnification 400×.

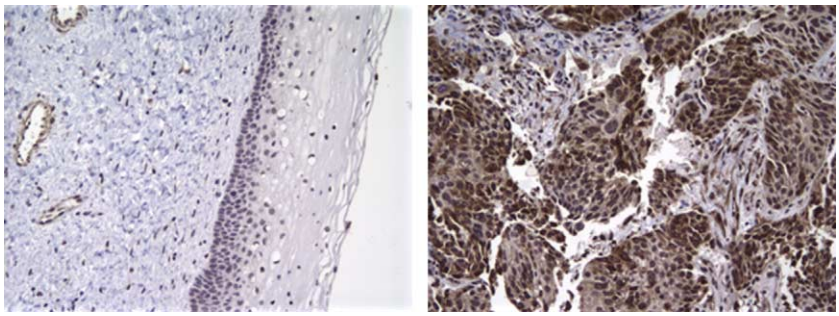

Fig. 5. Representative immunohistochemical staining for PTGES markers of one paraffin-embedded CVX specimen and one NCK specimen. NCK (left panel) showed negative staining for PTGES while CVX 1 (right panel) showed diffuse intense positivity for PTGES. Original magnification 400×.

pRb and p53 proteins (Quelle et al., 1995; Sano et al., 2002). Consistent with this hypothesis, an inverse relationship between the expression of p16 and p14ARF proteins and the presence of normal Rb and p53 in human cancer cells (Quelle et al., 1995; Sano et al., 2002), as well as an association between HPV infection and overexpression of p16 and p14ARF in cervical carcinoma and dysplasia, has been recently demonstrated (Khleif et al., 1996). Taken together, these data suggest that *CDKN2A* gene overexpression may represent a consistent genetic anomaly of HPV-infected cervical cancer cells. Furthermore, these results also suggest that *CDKN2A* gene products such as p16 and p14ARF (data not shown) may have significant potential as specific biomarkers to be targeted for diagnostic and/or prognostic purposes in cervical cancer (Murphy et al., 2003). Protein expression data obtained by flow cytometry with anti-p16 antibody on primary CVX cell lines and by immunohistochemistry on uncultured cervical tumor blocks further support this view.

In HPV-infected cervical tumors, the functional inactivation of pRb by E7 binding is thought to allow the accumulation of members of the E2F family of cellular transcription factors (Khleif et al., 1996), which signal the synthesis of enzymes required to drive the cell into S phase. In this model, E2F1 overexpression leads to an inhibition of cyclin D1-dependent kinase activity and induces the overexpression of the *CDKN2A* gene expression products (Khleif et al., 1996). Interestingly, high-risk HPV E7 oncoproteins have been previously shown to deregulate B-myb expression, a cell-cycle-regulated transcription factor the expression of which is also directed by an E2F-dependent transcriptional mechanism (Lam et al., 1994). Because B-myb is known to play an essential role in cell cycle progression (Joaquin and Watson, 2003), and expression of B-myb may bypass p53-induced p21-mediated G1 arrest (Lin et al., 1994), activation of the B-myb oncogene by E7 (Lam et al., 1994) may significantly contribute to the mitogenic activity of E7 in HPV-infected cervical tumors. Furthermore, because B-myb overexpression has been shown to overcome growth arrest associated with terminal differentiation (Bies et al., 1996) as well as cause a differentiation block in the presence of differentiation factors in human malignancies (Raschella et al., 1995), we speculate that B-myb overexpression in cervical cancer might be also involved in the rescue from senescence of HPV-transformed cervical cells as well as in the induction of a more aggressive cervical cancer phenotype. Our gene expression profile results are consistent with this view in that *CDKN2A*, *E2F1*, and *B-myb* genes were all found highly differentially expressed in HPV-infected tumors when compared to NCK.

Genomic imprinting is a mechanism by which a number of genes throughout the genome are monoallelically expressed according to their parental origin. Human mesoderm-specific transcript (MEST) is an imprinted gene expressed from the paternal allele and located on chromosome 7q32 (Pedersen et al., 1999). In this study, MEST was found to be one of the most highly differentially expressed gene in CVX compared to NCK. Of interest, loss of imprinting (LOI) or biallelic expression has been recently proposed as an important epigenetic mechanism for tumorigenesis in several human cancers including cervical cancer (Douc-Rasy et al., 1996; Kohda et al., 2001; Pedersen et al., 1999). To the best of our knowledge, however, MEST has not been previously linked to this disease. Importantly, in vitro treatment of tumor cells with 5-aza-2-deoxycytidine, a specific inhibitor of cytosine DNA methyl-transferase, has been reported to reverse LOI of insulin-like growth factor 2 (IGF2) and H19 genes, highlighting the potential of targeting aberrant tumor imprinting for therapeutic intervention (Barletta et al., 1997). Although the function of the MEST gene product is unknown, the putative protein shares homology with the α/β hydrolase family, which also includes the lysosomal enzyme cathepsin A (Kaneko-Ishino et al., 1995). This may suggest a possible role of MEST in the degradation of the extracellular matrix in the invasive state of cervical tumors.

Forkhead box (FOX) proteins constitute an extensive family of transcription factors, which share homology in the winged helix DNA binding domain (Clark et al., 1993) and which have been shown to play important roles in regulating the expression of genes involved in cell growth, proliferation, and transformation (Kaestner et al., 2000). Elevated FOXM1 levels have been found in numerous human tumors (Korver et al., 1997; Yao et al., 1997; Ye et al., 1997), suggesting that FOXM1 is required for cellular

proliferation in human cancer cells. However, the functional importance of this gene family in normal keratinocyte physiology and cervical cancer remains poorly understood. In our analysis, the *FOXM1* gene was found to be one of the most highly differentially expressed genes in CVX, with over sevenfold up-regulation relative to NCK. Because FOXM1 overexpression in human keratinocytes has been suggested to contribute to cell transformation and to be one of the mechanisms exerting a mitogenic effect on basal keratinocytes, leading to the development of basal cell cancer (The et al., 2002), it seems likely that FOXM1 overexpression may contribute to HPV-induced keratinocyte transformation and the development of cervical cancer. Although further work will be necessary to validate this hypothesis, inhibition of FOXM1 function might be a possible target for cervical anticancer therapies (Ruiz et al., 2002).

Prostaglandin E_2 synthase (PTGES) is a stimulus-inducible enzyme that functions downstream of cyclooxygenase (COX-2) in the PGE_2-biosynthetic pathway. The biological actions of PGE_2 have been attributed to its interaction with G-protein-coupled seven-transmembrane domain receptors, which belong to the rhodopsin superfamily of serpentine receptors (Murakami et al., 2002). Substantial clinical, genetic, and biochemical evidence suggests that PGE_2 plays a crucial role in the development of human tumors such as colorectal cancer (Murakami et al., 2002). In addition, elevated levels of PGE_2 and COX-2 proteins have been detected in a variety of human epithelial tumors including cervical cancers (Sales et al., 2001). In this regard, enhanced synthesis of PGE_2 resulting from up-regulated *COX-2* gene expression has been shown to stimulate gene transcription, inhibit apoptosis, and increase the metastatic potential of epithelial cells by promoting angiogenesis (Murakami et al., 2002). Consistent with the role played by PGE_2 in the development and progression of a variety of human tumors, in this study PGES-1 was found to be one of the most highly differentially expressed gene in CVX compared to NCK. Importantly, tumors secreting large amounts of PGE_2 significantly suppress cellular immunity in human cancer patients (Balch et al., 1984; Huang et al., 1998). These findings, combined with our data, support the hypothesis that PGE_2 overexpression by cervical cancer cells may play an important negative role during tumor–host–immune system interactions and thus contribute to immunological evasion by HPV-infected tumors. Importantly, nonsteroidal anti-inflammatory drugs, which inhibit COX-2, have been reported to be effective novel therapies to reduce the incidence of colorectal cancer (Murakami et al., 2002). Taken together, these data suggest that investigations to determine whether PGES-1 may represent a novel pharmacological target for preventing or treating cervical cancer would be worthwhile.

Topoisomerase II (TOP2A) is a nuclear enzyme that modulates DNA topology during several metabolic processes and is required for the segregation of daughter chromosomes at the end of replication (Pommier, 1993). In addition, *TOP2A* gene expression in human tumor cells is clinically and pharmacologically important, being targeted by a number of anticancer agents, including etoposide, mitoxantrone, and doxorubicin, which are termed topoisomerase II poisons (Pommier, 1993). A relationship between expression of topoisomerase II isoforms and intrinsic sensitivity to TOP2A inhibitors has been reported in several human tumors (Asano et al., 1996; Houlbrook et al., 1995; Pommier, 1993). In our study, *TOP2A* gene was found to be one of the most highly differentially expressed gene in CVX with over fivefold up-regulation relative to NCK. These data are consistent with a previous report showing high expression of the *TOP2A* gene product in invasive squamous cervical cancer (Gibbons et al., 1997). Of interest, a functional interaction between TOP2A and retinoblastoma protein has been recently described in which underphosphorylated Rb inhibits TOP2A activity (Bhat et al., 1999). We are therefore tempting to speculate that, in analogy to other previously described genes found highly overexpressed in HPV-infected CVX compared to NCK, functional inactivation of pRb by E7 binding may result in the marked overexpression of the *TOP2A* gene detected by gene expression profiling. Whatever the mechanism involved in TOP2A overexpression in HPV16/18-infected cervical cancer, these results suggest that future work testing the clinical efficacy of DNA topoisomerase II inhibitors in invasive cervical cancer refractory to standard treatment modalities might be beneficial.

CD97 is a dimeric glycoprotein belonging to the secretin-receptor superfamily and is abundantly expressed in cells of hematopoietic origin (Jaspars et al., 2001). CD97 has an extended extracellular region with several N-terminal epidermal growth factor (EGF)-like domains, which mediate binding to decay accelerating factor (DAF/CD55), a regulatory protein of the complement cascade (Hamann et al., 1996; Jaspars et al., 2001). Of interest, CD97 was found to be one of the most highly differentially expressed genes in CVX when compared to NCK. Recently, high expression of CD97 has been reported in human anaplastic thyroid carcinomas and poorly differentiated adenocarcinomas of the gastrointestinal tract (Aust et al., 1997; Jaspars et al., 2001). To the best of our knowledge, however, CD97 has not been previously linked to cervical cancer. Despite the fact that the biological function of CD97 is still unknown, accumulating data on its structure and molecular characteristics suggest a potential function associated with adhesion and signal transduction (Jaspars et al., 2001). Furthermore, it is likely that binding of CD55 to CD97 overexpressing tumor cells might favor tumor cell survival by protecting them from complement-dependent lysis, thus enhancing the potential for immunological evasion.

Cyclins are a family of molecules that control the cell cycle by associating with activating cyclin-dependent kinases (cdks). Cyclin B1 is a component of the cdc2 that

it is normally expressed at very low level in the cell nucleus. It appears at S phase, peaks in expression at G2/M, and it is rapidly degraded at the end of mitosis by ubiquitination and targeting to the proteasome (King et al., 1994). Studies in different human tumors and cell lines including breast, lung, colorectal, lymphoma, leukemia, and melanoma have detected overexpression of cyclin B1 at both protein and mRNA level (Finn, 2003). Consistent with these observations, a high differential expression of cyclin B1 was consistently found in all CVX tested when compared to NCK. The abnormal cyclin B1 level previously found in human tumors has been shown to correlate with either mutation or deletion of p53 function (Yu et al., 2002). Thus, it is likely that the well-established inactivation of p53 function by the tight binding to HPV16/18 E6 oncoproteins in cervical cancer may be responsible for cyclin B1 overexpression. Of interest, cyclin B1 has recently been identified as a shared human epithelial tumor-associated antigen recognized by T cells (Finn, 2003; Kao et al., 2001). Furthermore, cyclin B1 overexpression in human tumors was found to correlate with the presence of cyclin B1-specific memory T cell responses in cancer patients' peripheral blood, suggesting that T cells may be directly primed in vivo (Finn, 2003; Kao et al., 2001). Taken together, these data suggest that, in addition to high-risk HPV E6 and E7 oncoproteins (Santin et al., 1999, 2002), the aberrant overexpression and overabundance of cyclin B1-derived peptides in tumor HLA class I molecules (Finn, 2003; Kao et al., 2001) might be exploited as adjunctive targets for therapeutic vaccine development against cervical cancer.

A large number of down-regulated (at least twofold) genes in CVX versus NCK such as transforming growth factor, beta 1, transforming growth factor alpha, CFLAR, serine proteinase inhibitors (SERPING1 and SERPINF1), cadherin 13, protease inhibitor 3, keratin 16, and tissue factor pathway inhibitor-2 (TFPI-2) have been identified in our analysis. Some of these genes are known tumor suppressor genes or encode proteins important for epithelial tissue homeostasis or that have been previously implicated in apoptosis, proliferation, adhesion, or tissue maintenance. Because of space limitations, we will not comment further upon the cluster of genes that showed down-regulation of the transcripts in invasive tumors.

In conclusion, several CVX-restricted markers have been identified through our analysis. Some of these genes have been recently identified as up-regulated in other microarrays reports (for example, v-myb, TOP2A, diubiquitin, MMP-11) (Alazawi et al., 2002; Chang and Laimins, 2000; Chen et al., 2003; Nees et al., 2001; Oh et al., 2001), further validating our criteria for determination of differentially expressed genes, but most of the genes detected represent novel findings. Many of these up-regulated genes are likely to represent the result of aberrant activation of a number of dominant pathways that derive from the functional inactivation of pRb and p53 proteins by HPV oncoproteins. It is our hope that some of the cervical tumor markers identified in this work may be readily used for early detection of dysplasia and/or disease recurrence as well as the development of novel therapies against cervical cancer refractory to standard treatment modalities.

Materials and methods

Establishment of CVX and NCK primary cell lines

A total of 15 primary cell lines (i.e., 11 CVX and 4 NCK) were established after sterile processing of the samples from surgical biopsies as previously described (Santin et al., 1999). Fresh tumor biopsies from patients diagnosed with frankly invasive stage IB–IIA cervical cancer (staged according to the F.I.G.O. operative staging system) were obtained at the time of surgery and/or staging through the Gynecologic Oncology Division and the Pathology Department, UAMS, under approval of the Institutional Review Board. Patient characteristics are described in Table 5. Radical abdominal hysterectomy and lymph node dissection for invasive cervical cancer were performed in all patients but one. Normal keratinocyte control samples (i.e., four primary keratinocyte cultures) were obtained from cervical biopsies of hysterectomy specimens from women diagnosed with benign disease and a previous report of a normal cytological evaluation. All fresh primary cell lines were collected for RNA extraction at a confluence of 60–80% after a minimum of two to a maximum of 15 passages in vitro without significant differences in the number of passages between normal cells and cancer cell lines. Purity of fresh cultures was tested by morphology, immunohistochemistry staining, and/or flow cytometry with antibodies against cytokeratins. Only primary cultures that had at least 90% viability and contained >99% epithelial cells were used for total RNA extraction. No patient received radiation therapy or chemotherapy before surgery or tissue biopsy. Briefly, single-cell suspensions were obtained by processing

Table 5
Patient characteristics

Case	Age	Stage	Histology	HPV type	Treatment
CVX-1[a]	54	IB	Squamous	16	Surgery
CVX-2	32	IB	Adenosquamous	16	Surgery
CVX-3	51	IB	Squamous	16	Radiation
CVX-4	49	IB	Squamous	16	Surgery
CVX-5	44	IIA	Squamous	16	Surgery
CVX-6	43	IB	Squamous	16	Surgery
CVX-7	26	IB	Adenocarcinoma	18	Surgery
CVX-8	46	IB	Adenocarcinoma	18	Surgery
CVX-9	31	IB	Adenosquamous	18	Surgery
CVX-10	36	IB	Adenosquamous	18	Surgery
CVX-11	49	IB	Adenocarcinoma	18	Surgery

[a] Tumor cell lines were derived from biopsy obtained from the cervix in all patients.

solid tumor samples under sterile conditions at room temperature. Viable tumor tissue was mechanically minced in RPMI 1640 to portions no larger than 1–3 mm^3 and washed twice with RPMI 1640. The portions of minced tumor were then placed into 250 ml flasks containing 30 ml of enzyme solution [0.14% collagenase type I (Sigma, St. Louis, MO) and 0.01% DNAse (Sigma, 2000 kU/mg)] in RPMI 1640, and incubated on a magnetic stirring apparatus either for 2 h at 37 °C or overnight at 4 °C. Enzymatically dissociated tumor was then filtered through 150 μm nylon mesh to generate a single cell suspension. The resultant cell suspension was then washed twice in RPMI 1640 plus 10% human AB serum (Gemini Bioproducts, Calabasas, CA) before being seeded in tissue culture flasks in serum-free keratinocyte medium, supplemented with 5 ng/ml epidermal growth factor and 35–50 μg/ml bovine pituitary extract (Invitrogen, Grand Island, NY) at 37 °C.

HPV genotyping

Sequence-specific primers for the E7 oncoproteins were used to confirm or exclude by PCR the presence of the HPV16 and/or HPV18 genotype in the 11 primary CVX and in the four primary NCK cultures used in this study. Briefly, for HPV16, 0.1–1 μg of each genomic DNA sample was amplified in a 50-μl reaction containing 0.3 μM of each of the individual primers (HPV16 E7: F 5′-ATG GAG ATA CAC CTA CAT TGC-3′; R 5′-GGT TTC TGA GAA CAG ATG GGG C-3′) in the presence of 1× PCR buffer, 2.5 μM MgCl2, 0.8 μM dNTPs, and 0.025U/μl U AmpliTaq DNA polymerase (Applied Biosystems, Foster City, CA). Amplifications were performed in the Applied Biosystems GeneAmp PCR System 2700 (Applied Biosystems) at 95 °C for 3 min, followed by 35 cycles of 95 °C for 30 s, 60 °C for 30 s, 72 °C for 1 min, and a final extension of 72 °C for 7 min. For HPV18, 0.1–1 μg of each genomic DNA sample was amplified in a 50-μl reaction containing 0.25 μM of each of the individual primers (HPV18 E7: F 5′-CAT GGA CCT AAG GCA ACA TTG C-3′; R 5′-CTG CTG GGA TGC ACA CCA CGG-3′) in the presence of 1× PCR buffer, 2.0 μM MgCl2, 1 μM dNTPs, and 0.025U/μl U AmpliTaq DNA polymerase (Applied Biosystems). Amplifications were performed in the Applied Biosystems GeneAmp PCR System 2700 (Applied Biosystems) at 95 °C for 5 min, followed by 35 cycles of 95 °C for 1 min, 63 °C for 30 s, 72 °C for 1 min, and a final extension of 72 °C for 7 min. The PCR products were stored at 4 °C before electrophoresis on a 2% agarose gel. Beta-tubulin gene amplification with the following primers: F 5′-CGC ATC AAC GTG TAC TAC AA-3′, R 5′-TAC GAG CTG GTG GAC TGA GA-3′ (0.25 μM of each primer), was used as a positive internal control. SiHa (HPV-16) and HeLa (HPV-18) cervical carcinoma cell lines DNA were used as a positive external control. HT-3 (HPV-negative) cell line DNA and a water template were used as negative controls. As described in Table 5, all 11 primary cervical cancers were shown to harbor HPV16 or HPV18. In contrast, none of the four primary cervical keratinocyte cultures was found infected with HPV16 or HPV18 (data not shown).

RNA purification and microarray hybridization and analysis

Detailed protocols for RNA purification, cDNA synthesis, cRNA preparation, and hybridization to the Affymetrix Human U133A GeneChip microarray were performed according to the manufacturer's protocols, as reported previously (Ross et al., 2003).

Data processing

All data used in our analyses were derived from Affymetrix 5.0 software. GeneChip 5.0 output files contain for each probe set a continuous-valued "signal" that represents the difference between the intensities of the sequence-specific perfect-match probes and corresponding mismatch probes in each set, and a "detection" classification of each signal as present, marginal, or absent as determined by the GeneChip 5.0 algorithm. Gene arrays were scaled to an average signal of 1500 for calculation of each probe set's mean fold change in signal between CVX and NCK samples. For statistical assessment of differential expression, each array was normalized to give a mean of 0 and variance of 1 after log2-transformation of signal calls.

Gene expression data analysis

Statistical analyses of the data were performed with the software packages SPSS10.0 (SPSS, Chicago, IL). Genes were selected for analysis based on detection and fold change. In each comparison, genes having "present" detection calls in more than half of the samples in the overexpressed gene group (i.e., at least 6 out of 11 tumor samples or in at least three out of four normal samples) were retained for statistical analysis if they showed greater than twofold change between groups. A total of 1354 genes were retained and subsequently subjected to the Wilcoxon rank-sum (WRS) test at alpha = 0.05. One-sided upper 99% confidence limits (99% confidence maxima) on the number and percent of false discoveries at each P value were calculated numerically by applying Newton's method to the null-hypothesis distribution in the manner described by Siegel et al. (2004).

Gene cluster/Treeview

Hierarchical clustering via the average linkage method using the centered correlation metric was used (Ross et al., 2003; Zhan et al., 2002). The dendrogram was constructed with a subset of genes from 22,215 probe sets present on the

microarray, whose expression levels varied the most among the 15 samples, and were thus most informative. For the hierarchical clustering shown in Fig. 1, only genes significantly expressed and whose average change in expression level was at least twofold were chosen. The expression value of each selected gene was renormalized to have a mean of zero.

Quantitative real-time PCR

q-RT-PCR was performed with an ABI Prism 7000 Sequence Analyzer using the manufacturer's recommended protocol (Applied Biosystems) to validate differential expression of selected genes in samples from all primary cell lines (11 CVX and 4 NCK). Each reaction was run in triplicate. The comparative threshold cycle (C_T) method was used for the calculation of amplification fold as specified by the manufacturer. Briefly, 5 μg of total RNA from each sample was reverse transcribed using SuperScript III first-strand cDNA synthesis (Invitrogen, Carlsbad, CA). Ten microliters of reverse-transcribed RNA samples (from 500 μl of total volume) was amplified by using the TaqMan Universal PCR Master Mix (Applied Biosystems) to produce PCR products specific for cyclin-dependent kinase inhibitor 2A (*CDKN2A/p16*), *v-Myb*, *PTGES*, and *TOP2A*. Primers specific for 18S ribosomal RNA and empirically determined ratios of 18S competimers (Applied Biosystems) were used to control for the amounts of cDNA generated from each sample. Primers for *v-Myb*, *PTGES*, and *TOP2A* were obtained from Applied Biosystems as assay on demand products. Assays ID were Hs00231158_m1 (*v-Myb*), Hs00610420_m1 (*PTGES*), and Hs00172214_m1 (*TOP2A*). *CDKN2A/p16* primers sequences were the following (F 5′-CCC AAA CGC ACC GAA TAG TTA C-3′; R 5′-ATT CCA ATT CCC CTG CAA ACT-3′). Differences in CVX from NCK in the q-RT-PCR expression data were tested using the Kruskal–Wallis nonparametric test. Spearman rank correlations were used to estimate the degree of association between the microarray and q-RT-PCR data for each of these four genes.

Flow cytometry

To validate microarray data on primary CVX and NCK at the protein level, *CDKN2A/p16* expression was evaluated by flow cytometric analysis. Briefly, primary cells were harvested, washed, and fixed with 2% paraformaldehyde in PBS for 20 min at room temperature. Cells were then washed and permeabilized by incubation in PBS plus 1% BSA and 0.5% saponin (S-7900, Sigma) for 15 min at room temperature. Cells were stained with FITC-conjugated p16 antibody reagent set [anti-p16 (IgG1K) and isotype control antibodies (mouse IgG1K)] obtained from BD PharMingen (San Diego, CA). After staining, cells were washed twice with PBS plus 1% BSA and 0.5% saponin, once with PBS plus 0.5% BSA, and fixed a second time with 2% paraformaldehyde in PBS. Analysis was conducted with a FACScan, utilizing Cell Quest software (Becton Dickinson, San Jose, CA).

CDKN2A/p16 immunostaining of formalin-fixed tumor tissues

To evaluate whether the differential CDKN2A/p16 expression detected by flow cytometry on primary CVX cell lines was comparable to the expression of CDKN2A/p16 of cervical tumors from which the primary cell lines were derived, protein expression was evaluated by standard immunohistochemical staining on formalin-fixed tumor tissue from all surgical specimens (i.e., 11 CVX and 4 NCK controls). In addition, to validate our findings on a separate independent set of invasive cervical cancers, archival blocks derived from a further 10 patients harboring invasive cervical cancer were tested for CDKN2A/p16 expression. All 22 paraffin-embedded tumor tissues were also tested for the expression at protein level of PTGES. Study blocks were selected after histopathologic review by a surgical pathologist. The most representative hematoxylin- and eosin-stained block sections were used for each specimen. Sections (4 μm thick) were cut from formalin-fixed, paraffin-embedded samples, and mounted on charged slides. Sections were deparaffinized in xylene and rehydrated through graded alcohol to distilled water. Antigen retrieval was performed using Dako Target Retrieval Citrate Buffer solution (pH 6.0) in a Decloaking Chamber (Biocare Medical) for 20 min and cooled to room temperature for 30 min following the retrieval process. The slides were then rinsed in running distilled water and placed in Dako TBS with Tween (TBST) buffer solution. Endogenous peroxidase activity was blocked by incubating the slides in Dako hydrogen peroxidase blocking solution for 10 min. The slides were rinsed in TBST and incubated for 30 min in 10% normal goat serum (Vector Laboratories) diluted in TBST to assist in blocking the protein. The slides were blotted and not rinsed prior to applying the primary antibody. The slides were incubated for 1 h with a mouse anti-human p16 antibody (BD Pharmingen) at a 1:75 dilution with Dako antibody diluent with background-reducing agents or rabbit polyclonal antihuman mPGES antiserum (Cayman Chemical, Ann Arbor, MI) AT A 1:1000 dilution (2% BSA in PBS) for 18 h at 4 °C. The slides were rinsed in TBST and the secondary biotinylated goat anti-mouse antibody or biotinylated anti-rabbit antibody was added at a dilution of 1:400 in TBST for 30 min. The slides were again rinsed in TBST. The avidin–biotin complex (Vectastain Elite ABC Kit, Vector Laboratories) was applied and incubated for 30 min. Slides were developed in DAB + chromogen (DakoCytomation) for 3 min and rinsed in distilled water. Finally, the slides were counterstained for 2 min in hematoxylin 2 (Richard-Allan Scientific) and mounted and coverslipped. The intensity of staining was graded as negative (staining not greater than

negative control), 1+ (weak positivity), 2+ (focal intense positivity), and 3+ (diffuse intense positivity).

Acknowledgments

Supported in part by grants from the Angelo Nocivelli and the Camillo Golgi foundation, Brescia, Italy, and the Istituto Superiore di Sanita'(ISS) Rome, Italy.

References

Alazawi, W., Pett, M., Arch, B., Scott, L., Freeman, T., Stanley, M.A., Coleman, N., 2002. Changes in cervical keratinocyte gene expression associated with integration of human papillomavirus 16. Cancer Res. 62, 6959–6965.

Asano, T., An, T., Mayes, J., Zwelling, L.A., Kleinerman, E.S., 1996. Transfection of human topoisomerase II alpha into etoposide-resistant cells: transient increase in sensitivity followed by down-regulation of the endogenous gene. Biochem. J. 319, 307–313.

Aust, G., Eichler, W., Laue, S., Lehmann, I., Heldin, N.E., Lotz, O., Scherbaum, W.A., Dralle, H., Hoang-Vu, C., 1997. CD97: a dedifferentiation marker in human thyroid carcinomas. Cancer Res. 57, 1798–1806.

Balch, C.M., Dougherty, P.A., Cloud, G.A., Tilden, A.B., 1984. Prostaglandin E2-mediated suppression of cellular immunity in colon cancer patients. Surgery 95, 71–77.

Barletta, J.M., Rainier, S., Feinberg, A.P., 1997. Reversal of loss of imprinting in tumor cells by 5-aza-2′-deoxycytidine. Cancer Res. 57, 48–50.

Bhat, U.G., Raychaudhuri, P., Beck, W.T., 1999. Functional interaction between human topoisomerase IIalpha and retinoblastoma protein. Proc. Natl. Acad. Sci. U.S.A. 96, 7859–7864.

Bies, J., Hoffman, B., Amanullah, A., Giese, T., Wolff, L., 1996. B-Myb prevents growth arrest associated with terminal differentiation of monocytic cells. Oncogene 12, 355–363.

Bosch, F.X., Lorincz, A., Munoz, N., Meijer, C.J., Shah, K.V., 2002. The causal relation between human papillomavirus and cervical cancer. J. Clin. Pathol. 55, 244–265.

Chang, Y.E., Laimins, L.A., 2000. Microarray analysis identifies interferon-inducible genes and Stat-1 as major transcriptional targets of human papillomavirus type 31. J. Virol. 74, 4174–4182.

Chen, Y., Miller, C., Mosher, R., Zhao, X., Deeds, J., Morrissey, M., Bryant, B., Yang, D., Meyer, R., Cronin, F., Gostout, B.S., Smith-McCune, K., Schlegel, R., 2003. Identification of cervical cancer markers by cDNA and tissue microarrays. Cancer Res. 63, 1927–1935.

Clark, K.L., Halay, E.D., Lai, E., Burley, S.K., 1993. Co-crystal structure of the HNF-3/fork head DNA-recognition motif resembles histone H5. Nature 364, 412–420.

Douc-Rasy, S., Barrois, M., Fogel, S., Ahomadegbe, J.C., Stehelin, D., Coll, J., Riou, G., 1996. High incidence of loss of heterozygosity and abnormal imprinting of H19 and IGF2 genes in invasive cervical carcinomas. Uncoupling of H19 and IGF2 expression and biallelic hypomethylation of H19. Oncogene 12, 423–430.

Finn, O.J., 2003. Premalignant lesions as targets for cancer vaccines. J. Exp. Med. 198, 1623–1626.

Gibbons, D., Fogt, F., Kasznica, J., Holden, J., Nikulasson, S., 1997. Comparison of topoisomerase II alpha and MIB-1 expression in uterine cervical squamous lesions. Mod. Path. 10, 409–413.

Hamann, J., Vogel, B., van Schijndel, G.M., van Lier, R.A., 1996. The seven-span transmembrane receptor CD97 has a cellular ligand (CD55, DAF). J. Exp. Med. 184, 1185–1189.

Houlbrook, S., Addison, C.M., Davies, S.L., Carmichael, J., Stratford, I.J., Harris, A.L., Hickson, I.D., 1995. Relationship between expression of topoisomerase II isoforms and intrinsic sensitivity to topoisomerase II inhibitors in breast cancer cell lines. Br. J. Cancer 72, 1454–1461.

Huang, M., Stolina, M., Sharma, S., Mao, J.T., Zhu, L., Miller, P.W., Wollman, J., Herschman, H., Dubinett, S.M., 1998. Non-small cell lung cancer cyclooxygenase-2-dependent regulation of cytokine balance in lymphocytes and macrophages: up-regulation of interleukin 10 and down-regulation of interleukin 12 production. Cancer Res. 58, 1208–1216.

Jaspars, L.H., Vos, W., Aust, G., Van Lier, R.A., Hamann, J., 2001. Tissue distribution of the human CD97 EGF-TM7 receptor. Tissue Antigens 57, 325–331.

Jemal, A., Murray, T., Samuels, A., Ghafoor, A., Ward, E., Thun, M.J., 2003. Cancer statistics. CA Cancer J. Clin. 53, 5–26.

Joaquin, M., Watson, R.J., 2003. Cell cycle regulation by the B-Myb transcription factor. Cell. Mol. Life Sci. 60, 2389–2401.

Kaestner, K.H., Knochel, W., Martinez, D.E., 2000. Unified nomenclature for the winged helix/forkhead transcription factors. Genes Dev. 14, 142–146.

Kaneko-Ishino, T., Kuroiwa, Y., Miyoshi, N., Kohda, T., Suzuki, R., Yokoyama, M., Viville, S., Barton, S.C., Ishino, F., Surani, M.A., 1995. Peg1/Mest imprinted gene on chromosome 6 identified by cDNA subtraction hybridization. Nat. Genet. 11, 52–59.

Kao, H., Marto, J.A., Hoffmann, T.K., Shabanowitz, J., Finkelstein, S.D., Whiteside, T.L., Hunt, D.F., Finn, O.J., 2001. Identification of cyclin B1 as a shared human epithelial tumor-associated antigen recognized by T cells. J. Exp. Med. 194, 1313–1323.

Khleif, S.N., DeGregori, J., Yee, C.L., Otterson, G.A., Kaye, F.J., Nevins, J.R., Howley, P.M., 1996. Inhibition of cyclin D-CDK4/CDK6 activity is associated with an E2F-mediated induction of cyclin kinase inhibitor activity. Proc. Natl. Acad. Sci. U.S.A. 93, 4350–4354.

King, R.W., Jackson, P.K., Kirschner, M.W., 1994. Mitosis in transition. Review. Cell 79, 563–571.

Kohda, M., Hoshiya, H., Katoh, M., Tanaka, I., Masuda, R., Takemura, T., Fujiwara, M., Oshimura, M., 2001. Frequent loss of imprinting of IGF2 and MEST in lung adenocarcinoma. Mol. Carcinog. 31, 184–191.

Korver, W., Roose, J., Clevers, H., 1997. The winged-helix transcription factor Trident is expressed in cycling cells. Nucleic Acids Res. 25, 1715–1719.

Lam, E.W., Morris, J.D., Davies, R., Crook, T., Watson, R.J., Vousden, K.H., 1994. HPV16 E7 oncoprotein deregulates B-myb expression: correlation with targeting of p107/E2F complexes. EMBO J. 13, 871–878.

Landoni, F., Maneo, A., Colombo, A., Placa, F., Milani, R., Perego, P., Favini, G., Ferri, L., Mangioni, G., 1997. Randomised study of radical surgery versus radiotherapy for stage Ib–IIa cervical cancer. Lancet 350, 535–540.

Lin, D., Fiscella, M., O'Connor, P.M., Jackman, J., Chen, M., Luo, L.L., Sala, A., Travali, S., Appella, E., Mercer, W.E., 1994. Constitutive expression of B-myb can bypass p53-induced Waf1/Cip1-mediated G1 arrest. Proc. Natl. Acad. Sci. U.S.A. 91, 10079–10083.

Murakami, M., Nakatani, Y., Tanioka, T., Kudo, I., 2002. Prostaglandin E synthase. Prostaglandins Other Lipid Mediators 68–69, 383–399.

Murphy, N., Ring, M., Killalea, A.G., Uhlmann, V., O'Donovan, M., Mulcahy, F., Turner, M., McGuinness, E., Griffin, M., Martin, C., Sheils, O., O'Leary, J.J., 2003. 16INK4A as a marker for cervical dyskaryosis: CIN and cGIN in cervical biopsies and ThinPrep smears. J. Clin. Pathol. 56, 56–63.

Nees, M., Geoghegan, J.M., Hyman, T., Frank, S., Miller, L., Woodworth, C.D., 2001. Papillomavirus type 16 oncogenes downregulate expression of interferon-responsive genes and upregulate proliferation-associated and NF-kappaB-responsive genes in cervical keratinocytes. J. Virol. 75, 4283–4296.

Oh, S.T., Kyo, S., Laimins, L.A., 2001. Telomerase activation by human papillomavirus type 16 E6 protein: induction of human telomerase reverse transcriptase expression through Myc and GC-rich Sp1 binding sites. J. Virol. 75, 5559–5566.

Pedersen, I.S., Dervan, P.A., Broderick, D., Harrison, M., Miller, N., Delany, E., O'Shea, D., Costello, P., McGoldrick, A., Keating, G., Tobin, B., Gorey, T., McCann, A., 1999. Frequent loss of imprinting of PEG1/MEST in invasive breast cancer. Cancer Res. 59, 5449–5451.

Pommier, Y., 1993. Topoisomerase I and II in cancer chemotherapy: update and perspectives. Cancer Chemother. Pharmacol. 32, 103–108.

Quelle, D.E., Zindy, F., Ashmun, R.A., Sherr, C.J., 1995. Alternative reading frames of the INK4a tumor suppressor gene encode two unrelated proteins capable of inducing cell cycle arrest. Cell 83, 993–1000.

Raschella, G., Negroni, A., Sala, A., Pucci, S., Romeo, A., Calabretta, B., 1995. Requirement of b-myb function for survival and differentiative potential of human neuroblastoma cells. J. Biol. Chem. 270, 8540–8545.

Ross, M.E., Zhou, X., Song, G., Shurtleff, S.A., Girtman, K., Williams, W.K., Liu, H.C., Mahfouz, R., Raimondi, S.C., Lenny, N., Patel, A., Downing, J.R., 2003. Classification of pediatric acute lymphoblastic leukemia by gene expression profiling. Blood 102, 2951–2959.

Ruiz, I., Altaba, A., Sanchez, P., Dahmane, N., 2002. Gli and hedgehog in cancer: tumours, embryos and stem cells. Nat. Rev., Cancer 2, 361–372.

Sales, K.J., Katz, A.A., Davis, M., Hinz, S., Soeters, R.P., Hofmeyr, M.D., Millar, R.P., Jabbour, H.N., 2001. Cyclooxygenase-2 expression and prostaglandin E(2) synthesis are up-regulated in carcinomas of the cervix: a possible autocrine/paracrine regulation of neoplastic cell function via EP2/EP4 receptors. J. Clin. Endocrinol. Metab. 86, 2243–2249.

Sano, T., Masuda, N., Oyama, T., Nakajima, T., 2002. Overexpression of p16 and p14ARF is associated with human papillomavirus infection in cervical squamous cell carcinoma and dysplasia. Pathol. Int. 52, 375–383.

Santin, A.D., Hermonat, P.L., Ravaggi, A., Chiriva-Internati, M., Zhan, D., Pecorelli, S., Parham, G.P., Cannon, M.J., 1999. Induction of human papillomavirus-specific CD4(+) and CD8(+) lymphocytes by E7-pulsed autologous dendritic cells in patients with human papillomavirus type 16- and 18-positive cervical cancer. J. Virol. 73, 5402–5410.

Santin, A.D., Bellone, S., Gokden, M., Cannon, M.J., Parham, G.P., 2002. Vaccination with HPV-18 E7-pulsed dendritic cells in a patient with metastatic cervical cancer. N. Engl. J. Med. 346, 1752–1753.

Siegel, E.R., Spencer, T., Parrish, R.S., 2004. Controlling false discovery when planning microarray experiments. 2003 Proceedings of the American Statistical Association. Mira Digital Publishing, St. Louis, MO, pp. 3897–3899.

The, M.T., Wong, S.T., Neill, G.W., Ghali, L.R., Philpott, M.P., Quinn, A.G., 2002. FOXM1 is a downstream target of Gli1 in basal cell carcinomas. Cancer Res. 62, 4773–4780.

Yao, K.M., Sha, M., Lu, Z., Wong, G.G., 1997. Molecular analysis of a novel winged helix protein, WIN. Expression pattern, DNA binding property, and alternative splicing within the DNA binding domain. J. Biol. Chem. 272, 19827–19836.

Ye, H., Kelly, T.F., Samadani, U., Lim, L., Rubio, S., Overdier, D.G., Roebuck, K.A., Costa, R.H., 1997. Hepatocyte nuclear factor 3/fork head homolog 11 is expressed in proliferating epithelial and mesenchymal cells of embryonic and adult tissues. Mol. Cell. Biol. 17, 1626–1641.

Yu, M., Zhan, Q., Finn, O.J., 2002. Immune recognition of cyclin B1 as a tumor antigen is a result of its overexpression in human tumors that is caused by non-functional p53. Mol. Immunol. 38, 981–987.

Zhan, F., Tian, E., Bumm, K., Smith, R., Barlogie, B., Shaughnessy Jr., J., 2002. Gene expression profiling of human plasma cell differentiation and classification of multiple myeloma based on similarities to distinct stages of late-stage B-cell development. Blood 99, 1745–1757.